Characterization of a Li-ion Battery Based Stand-alone a-Si Photovoltaic System

A thesis submitted to the
Graduate School of Natural and Applied Sciences

by

Mehdi Hamid Vishkasougheh

in partial fulfillment for the
degree of Master of Science

in
Industrial and Systems Engineering

This is to certify that we have read this thesis and that in our opinion it is fully adequate, in scope and quality, as a thesis for the degree of Master of Science in Industrial and Systems Engineering.

APPROVED BY:

Assoc. Prof. B. Tunaboylu ..... (Thesis Advisor)

Assoc. Prof. O Öztürk .....

Asst. Prof. M. Tanyeri .....

This is to confirm that this thesis complies with all the standards set by the Graduate School of Natural and Applied Sciences of İstanbul Şehir University:

DATE OF APPROVAL: 7 April 2014

SEAL/SIGNATURE:

Declaration of Authorship

I, Mehdi HAMID VISHKASOUGHEH, declare that this thesis titled, 'Characterization of a Li-ion Battery Based Stand-alone a-Si Photovoltaic System' and the work presented in it are my own. I confirm that:

- This work was done wholly or mainly while in candidature for a research degree at this University.
- Where any part of this thesis has previously been submitted for a degree or any other qualification at this University or any other institution, this has been clearly stated.
- Where I have consulted the published work of others, this is always clearly attributed.
- Where I have quoted from the work of others, the source is always given. With the exception of such quotations, this thesis is entirely my own work.
- I have acknowledged all main sources of help.
- Where the thesis is based on work done by myself jointly with others, I have made clear exactly what was done by others and what I have contributed myself.

Signed: Mehdi Hamid

Date: 18.04.2014

Characterization of a Li-ion Battery Based Stand-alone a-Si Photovoltaic System

Mehdi Hamid Vishkasougheh

Abstract

The number of photovoltaic (PV) system installations is increasing rapidly. As more people learn about this versatile and often cost-effective power option, this trend will accelerate. This document presents a recommended design for a battery based stand-alone photovoltaic system (BSPV). BSPV system has the ability to have application in different areas. These include warning signals, lighting, refrigeration, communication, residential water pumping, remote sensing, and cathodic protection. The presented calculation method gives a proper idea for a system sizing technique. Based on application load, different scenarios are possible for designing a BSPV system. In this study a battery based stand-alone system was designed. For the electricity generation part, A high efficiency silicon solar cells with a hetro-junction microcrystalline intrinsic thin layer was investigated. However, lack of availabilty of this type of panel made us to choose amorphous silicon panels. The electricity generation part is three a-Si panels, which are connected in parallel, and for the storage part LFP (Lithium Iron Phosphate) battery was used. The high power LFP battery packs are 40 cells each 8S5P (configured 8 series 5 parallel). Each individual pack weighs 0.5 kg and is 25.6V. In order to evaluate the efficiency of a-Si panels with respect to the temperature and the solar irradiation, cities of Istanbul, Ankara and Adana in Turkey were selected. Temperature and solar irradiation were gathered from reliable sources and by using translation equations current and voltage output of panels were calculated. As a result of these calculations, current and energy outputs were camputed by considering an average efficient solar irradiation time value per day in Turkey. The calculated power values were inserted to a battery cycler system, and the behavior of high power LFP batteries in a time sequence of 7.2h was evaluated. The charging and discharging cycles were obtained and their behavior was discussed. According to the results, Istanbul has the lowest number of peak month's energy, it followed by Ankara, and ultimately Adana has the highest number of peak months and energy storage. It was observed during the tests that, values up to 4 A was discharged by battery packages in a full discharge cycle depending on application and required load. This amount can be different depending on application and required load.

Keywords: Photovoltaics, Amourphous Silicon, Li-ion Battery

Tekil Si Fotovoltaik Sistem Temelli, Li-iyon Bataryanın Karakterizasyonu

Mehdi Hamid Vishkasougheh

Öz

Fotovoltaik (PV) sistemlerin kurulumu hızlıca artmaktadır. Çok amaçlı ve genellikle uygun maliyetli bu güç seçeneğini daha fazla insanın öğrenmesi, bu sistemlere yönelimi ivmelendirecektir. Bu çalışma, batarya temelli tekil fotovoltaik sistemler ($BSPV$) için tavsiye edilen bir tasarımı sunmaktadır. BSPV sistemi faklı alanlarda uygulanabilme kabiliyetine sahiptir. Bu uygulamalar, uyarı sinyallerinin elde edilmesi, aydınlatma, soğutma, iletişim, evsel su temini, uzaktan algılama ve katodik korumadır. Bu çalışmada sunulan hesaplama, sistem boyutlandırma tekniği için uygun bir yöntemi içerir. Uygulama yüküne bağlı BSPV sisteminin tasarımı, fakı senaryolar için mümkündür. Bu çalışmada batarya temelli tekil sistem tasarlanmıştır. Elektrik üretimi bölümü için, farklı eklemli, mikrokristal yapıda, intrinsik ince film, yüksek verimlilikte, silikon güneş pilleri araştırılmıştır. Elektrik üretimi ile ilgili bölümde 3 adet Si panel paralel olarak bağlanmıştır ve depolama bölümünde, LFP ($LityumDemirFosfat$) batarya kullanılmıştır. Yüksek güç çıktısına sahip, LFP batarya paketi her biri 8S5P (8 hücre seri, 5 hücre paralel bağ lanarak) olan 40 hücreden oluşmuştur. Her bir paket 0.5 kg ağırlığa sahiptir ve 25.6 voltur. Si panellerin verimini, sıcaklık ve güneş ışınlarının yayılımına göre değerlendirmek için Türkiye'de İstanbul, Ankara ve Adana şehirleri seçilmiştir. Sıcaklık ve güneş ışınlarının yayılımı güvenilir bir kaynaktan alınmış ve çevrim eşitlikleri kullanılarak panellerin akım ve gerilim çıktıları hesaplanmıştır. Bu hesaplamaların sonuçlarına göre akım ve enerji çıktıları, bir günlük ortalama etkin güneş ışınlarının yayılım değerinin dikkate alınmasıyla elde edilmiştir. Hesaplanan güç değerleri batarya çevrim sistemine yerleştirilmiş ve 7.2 saatlik arda arda çevrimlerle yüksek güce sahip LFP bataryaların davranışı değerlendirilmiştir. Şarj ve deşarj çevrimleri elde edilmiş ve bunların davranışlarıt artışılmıştır. Sonuçlara göre; İstanbul enerji değerlerine göre en az sayıda pik aylara sahipken, Ankara onu izlemiş ve nihayetinde Adana'nın en yüksek pik aylarına ve enerji depolama sayılarına sahip olduğu tespit edilmiştir. Testler boyunca, gerekli yük miktarına ve uygulamaya bağlı olarak tam bir deşarj çevriminde 4 A'lik akım batarya paketinden deşarj edilmiştir. Bu miktar uygulamaya ve gerekli yüke bağlı olarak farklılık gösterebilir.

Anahtar Sözcükler: Fotovoltaik, Amorf Silikon, Li-iyon Batarya

I dedicate this thesis to Prof. Bahadır Tunaboylu who supported me each step of the way.

Acknowledgments

I acknowledge Istanbul Sehir University, the Academic Writing Center of the university, and TÜBİTAK Energy Institute for all their support.

Contents

List of Figures

List of Tables

Abbreviations

V	**Voltage**
h	**h**our
m	**m**eter
STC	**S**tandard **T**est **C**ondition
V_{oc}	**O**pen **C**ircuit **V**oltage
HIT	**H**etero-junction **I**ntrinsic **T**hin-layer
FF	**F**ill **F**actor
TCO	**T**ransparent **C**onductive **O**xide
J_{sc}	**S**hort **C**ircuit **C**urrent
μ**c-Si**	**M**icro-crystalline **S**ilicon
H	**H**ydrogen
PV	**P**hoto**V**oltaic
W	**W**att
DC	**D**irect **C**urrent
LGBG	**L**aser **G**rooved **B**uried **G**rid
MW	**M**ega**W**att
BIPV	**B**uilding **I**ntegrated **P**hotovoltaic
a-Si	**A**morphus **S**ilicon
RCA	**R**adio **C**orporation **A**merica
Li	**L**ithium
LMO	**L**ithium **M**anganse **O**xide
LFP	**L**ithium **I**ron **P**hosphate
NMC	**L**ithuim **N**ickel **M**anganese **C**obalt Oxide
NCA	**L**ithium **N**ickel **C**obalt **A**luminum oxide
LTO	**L**ithium **T**itanate **O**xide

DDP	**D**eep **D**ischarge **P**rotection
BTS	**B**attery **T**est **S**ystem
UBT	**U**niversal **B**attery **T**ester

Physical Constants

Planck's Constant	$\hbar$	=	$6.6261 \times 10^{-34}\ m^2$ kg/s
Current Coefficient	a	=	%0.9
Voltage Coefficient	β	=	%-0.33
Curve correction factor	k	=	0

Symbols

Symbol	Name	Unit
υ	Frequency	s^{-1}
P	power	W (Js^{-1})
α	Optical Absorbtion Coefficient	m^{-1}
G	Irradition	$KWhm^{-2}$
T	Temperature	C
I_{sc}	Short Circuit Current	A

Chapter 1

Introduction

1.1 Background of Photovoltaics

Photovoltaics (PV) are an innovation producing direct current (DC) electrical power measured in Watts (W) from semiconductors when they are exposed to photons. Whenever light is shining on a solar cell (the name for the single PV component), it creates electricity. However, when the light stops shining, the electricity generation stops. Unlike batteries, solar cells never need recharging [1].

Regularly, the advantages and disadvantages of photovoltaics are almost fully the inverse of the currently accepted fossil-fuel power plants. For instance, fossil-fuel plants have weaknesses of an extensive variety of environmentally hazardous emissions for example large amount of carbon dioxide emissions that cause health risks, many parts that deteriorate because of wear that make us to have regular maintenace schedule, high and increasing fuel costs which makes high amount of capital investment, non-modular (not deployable in small increments), and have a negative public opinion towards them. Also in case of fuel energy, transportation cost and delivery delay in harsh weather conditions are other issues that need to be considered. Photovoltaics do not have any of these issues. The two characteristics that both PV and fossil fuel powered plants share are they are exceptionally dependable and they both fail to have the benefit of electricity storage [1].

In general advantages of photovoltaics are: in-finite source of energy, no global climate pollution, cost effective, high reliability, modular, quick installation, capability of being install into new buildings, possible match between demand and useage, user friendliness

and quiet, year round continues and unlimited operation with moderate cost. However, there are some disadvantages like relatively low-density energy, high installation costs, poor reliability of auxilary of system element balance, not abundent in commercial market and lack of storage system.

The troubles of PV are nontechnical, and are generally related to cost and structure. These flaws are in part adjusted for by an exceptionally high public acceptance and awareness of the environmental offsets. Throughout the late 1990s, the common development rate of PV has been running at over 33% per annum. In the following years the development processes have been continued. As long as the technology and efficiency increase, number of production increase and this will influence directly on the final cost of the product.

1.1.1 Physical Theory of PV

What is the physical premise of PV operation? Solar cells are made of materials called semiconductors, which have weakly bonded electrons possessing a band of energy called the valence band [1]. When energy surpasses a certain limit, called the "band gap energy", connected to a valence electron, the bonds are broken and the electron is "free" to move around in another energy band called the conduction band where it can "conduct" power through the material. Accordingly, the free electrons in the conduction band are differentiated from the valence band by the band gap (measured in units of electron volts or ev). This energy required to free the electron might be supplied by photons, which are particles of light. Photons from sunlight, which their energy is more than band gap energy creates free electrons. These free electrons can move to conduction band. In this stage collectors send these electrons to the outside circuit in order to produce electric power. The electrons lose their energy by doing work in the outer circuit, for example pumping water, turning a fan, driving a sewing machine, a light, or a workstation. The electrons return to the valence band by the outside circuit with the same energy the started [1]. Figure1.1 shows a schematic view of how a solar cell operation when it is confronted to sunlight.

Sunshine is a range of photons distributed over a range of energy. Photons whose energy is more than the band gap (the threshold energy) can excite electrons from the valence to the conduction band where they can repeat the process and create electricity. Photons

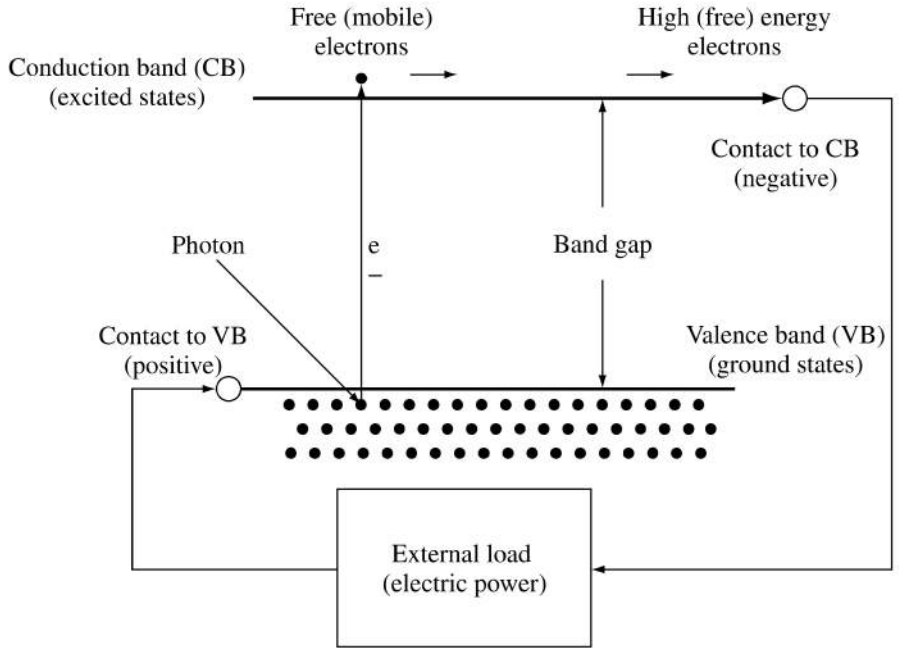

FIGURE 1.1: Schematic of a solar cell (source [1])

with energy less than the energy gap are not able to excite the free electrons. Rather, this energy moves through the solar cell and is absorbed at the back as heat. Solar cells in immediate daylight could be to some degrees (20-30 ∘C) warmer than the ambient air temperature. Therefore PV units can create power without working at high temperature and without moving parts[1].

1.2 History of Photovoltaics

The history of photovoltaics goes back to the nineteenth century. The foremost, purpose-made PV unit was by Fritts [11] in 1883. He liquefied Se into a flimsy sheet on a metal substrate and pressed an Au-leaf film as the top contact. It was about 30 cm^2 in size. He noted, "the current, if not wanted immediately, can be either stored where produced, in storage batteries, or transmitted a distance and there used."

Major steps toward commercialising PV cells were taken in 1940s and 1950s when Czochralski developed pure crystalline silicon production process. In 1954 at Bell labaratory first crystalline Si PV cell was developed with efficiency of 4% [12].

Additionally as a result of Cherry conference in 1973, photovoltaic received US government support. At the end of the same year, the first oil embargo made a shocking wave through the industrialized world. This made most of the governments support renewable energy and solar cell energy. This was the beginning of modern age of photovoltaics.

1.3 Amorphous Silicon

Since the porpuse of this research is using a-Si as a PV material for designing a battery based stand alone PV system, therefore, in this section different aspects of a-Si is discussed.

Crystalline semiconductors are prominently known, incorporating silicon (the basis of the integrated circuits used in modern electronics), Ge (the material of the first transistor), GaAs and the other III-V components (the basis for many light emitters), and CdS (frequently utilized as a light sensor). In the crystals, the atoms are sorted in a nearly perfect order, in regular arrays or lattices. Clearly, the lattice must be regular with the underlying chemical bonding properties of the atoms. Case in point, a silicon atom structures have four covalent bonds to neighboring particles arranged symmetrically. This "tetrahedral" setup is consummately kept up in the "diamond" lattice of crystal silicon.

There are additionally various noncrystalline semiconductors. In these materials, the chemical bonding of particles is almost unaltered from that of crystals. In any case, small, dislocated variation in the angles between bonds impairs the overall lattice configuration. The primary economically important illustration was xerography [13] and [14], which exploited the photoconductivity of noncrystalline selenium.

On the other hand, solar cells require that photogenerated electrons and holes be separated by near modest electric fields that are "built-in" to the device, and selenium and numerous other noncrystalline semiconductors were determined as undesirable for making effective cells.

In the 1970s, in Dundee, Scotland, Walter Spear and Peter LeComber found that amorphous silicon manufactured by a "glow discharge" in silane (SiH4) gas had exceptionally

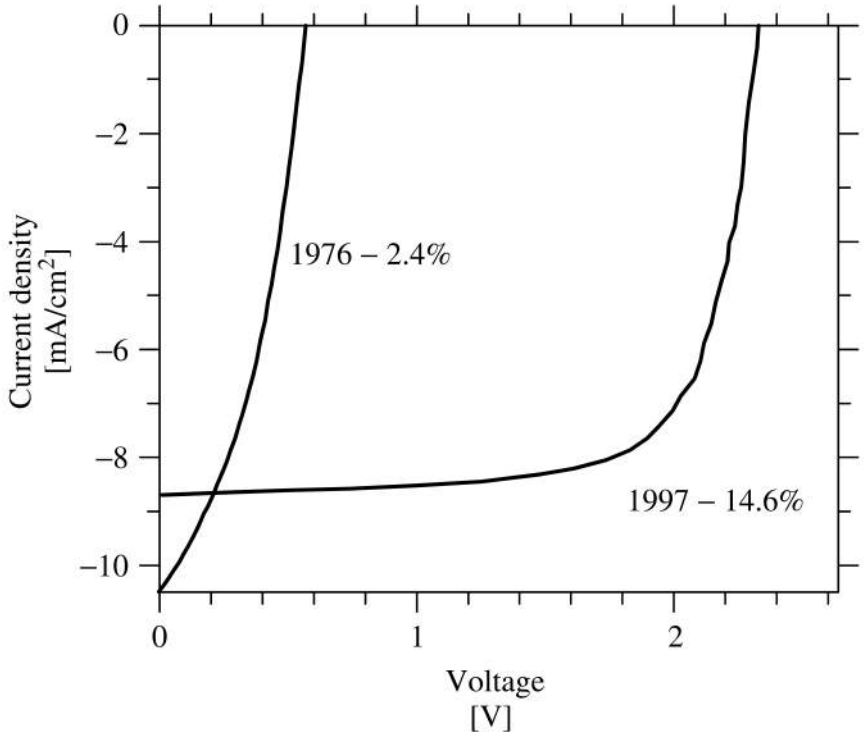

FIGURE 1.2: Density versus voltage under solar illumination for a single-junction a-Si solar cell (Carlson and Wronski [2]) and from a recent "triple-junction" cell (Yang, Banerjee, and Guha [3]).

suitable electronic characteristics; they were building on earlier work by Chittick, Sterling, and Adler [15]. Amorphous silicon was deposited as a thin film on substrates inserted into the silane gas discharge. Spear and LeComber stated in 1975 [16] that conductivity of amorphous silicon could be improved greatly either by blending some phosphine (PH3) gas or some diborane (B2H6) gas with the silane.

In 1976, he and Christopher Wronski described a solar cell based on amorphous silicon [2] with a solar conversion efficiency of about 2.4% (for historical discussion see References [17] and [18]). Carlson and Wronski's report of the current density against output voltage is introduced in Figure 1.2 (in addition to the curve from a significantly more efficient cell reported in 1997 [3]). As these researchers identified, the optoelectronic characteristics of amorphous silicon made by glow discharge (or "plasma deposition") are genuinely superior to the amorphous silicon thin films made, for example, by merely evaporating silicon.

After a few years of uncertainty, it seemed that plasma-deposited amorphous silicon had

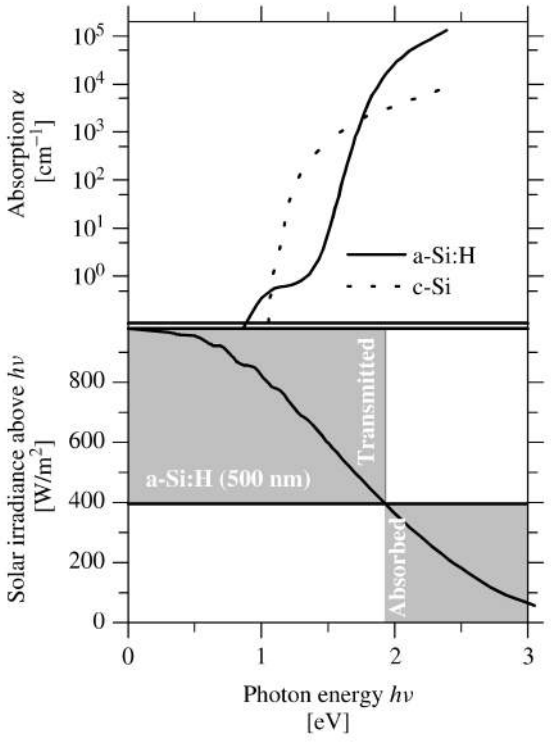

FIGURE 1.3: (Upper panel) Spectra of the optical absorption coefficient $\alpha(\hbar\nu)$ v.s. photon energy $\hbar\nu$ for c-Si and for a-Si:H. (Lower panel) Irradiance of photons in the solar spectrum with energies $\alpha(\hbar\nu)$or larger. (source: [4])

a meaningful amount of hydrogen atoms bonded into the amorphous silicon structure and that these hydrogen atoms were central to the enhancement of the electronic properties of the plasma deposited material [19]. As a result, the enhanced form of amorphous silicon has become known as hydrogenated amorphous silicon (or, more briefly, a-Si:H). Recently, numerous authors have stated the hydrogenated form with the term amorphous silicon, which acknowledges the fact that the unhydrogenated forms of amorphous silicon are only sporadically investigated nowadays.

Why was there this much interest about the a-Si solar cells produced by Carlson and Wronski? Firstly, the technology is rather modest and inexpensive in contrast with the technologies for growing crystals. In addition, the optical properties of a-Si are very encouraging for collecting solar energy. In Figure 1.3, the upper panel displays the spectrum for the optical absorption coefficients $\alpha(\hbar\nu)$ for amorphous silicon and for crystalline silicon [4]. In the lower panel is the spectrum of the "integrated solar irradiance" which is the intensity (in W/m^2) of the solar energy carried by photons above an energy threshold $\hbar\nu$.

These spectra are used to discover how much solar energy is absorbed by layers of variable thickness. The example in the figure is an a-Si:H layer with a thickness d = 500 nm. essentially all photons with energies larger than 1.9 eV (the energy at which $\alpha = 1/d$). Subsequently it is determined that how much solar irradiance lies above 1.9 eV. By assuming that the light reflection is minimized, around 420 W/m2 is found to be absorbed by the layer (the gray area labeled "absorbed"). Through such a layer $580W/m^2$of energy is transmitted. One might compare these energies with the results for c-Si, for which a 500-nm-thick layer absorbs less than $200W/m^2$. In order to absorb the energy same as the 500-nm a-Si:H layer, a c-Si layer should be much thicker. The reason is that much less material is required to make a solar cell from a-Si than from c-Si.

1.4 Types of Lithium-ion Batteries

In order to design a Li ion battery based stand alone a-Si PV system Li ion batteries should be investigated. For this study, Lithium Iron phosphate was applied. However a general overview about other types of Li battries is discussed in the following paragraph and Table 1.1.

There are different types of lithium-ion batteries. As there are numerous types of apple trees, so do also lithium-ion batteries vary and the difference is basically in the cathode materials. Moreover new materials are appearing in the anode to modify or replace graphite. Researchers prefer to name batteries by their chemical name and material used. Table 1.1 offers clarity by listing these batteries by their full name, chemical definition, abbreviations and short form. To complete the list of the recognized Li-ion batteries, the table also contains NCA and Li-titanate, two lesser-known members of the Li-ion family [9].

1.5 Lithium Iron Phosphate (LiFePO4) Battery

High demand load for oil, put so much pressure on energy world with considering recent concerns associated with environment like global warming. Issues like that make the application of clean and efficient energy production with renewable sources bolder than what it had been previously. Lead batteries and Ni-MH batteries lost their attraction

Table 1.1: Reference names for Li-ion batteries (Source: [9])

Chemical name	Material	Abbreviation	Short form	Notes
Lithium Cobalt Oxide Also Lithium Cobalate or lithium-ion-cobalt)	LiCoO2 (60% Co)	LCO	Li-cobalt	High capacity; for cell phone laptop, camera
Lithium Manganese Oxide Also Lithium Manganate or lithium-ion-manganese	LiMn2O4	LMO	Li-manganese, or spinel	Most safe; lower capacity than Li-cobalt but high specific power and long life. Power tools, e-bikes, EV, medical, hobbyist.
Lithium Iron Phosphate	LiFePO4	LFP	Li-phosphate	
Lithium Nickel Manganese Cobalt Oxide, also lithium-manganese-cobalt-oxide	LiNiMnCoO2 (10-20% Co)	NMC	NMC	
Lithium Nickel Cobalt Aluminum Oxide	LiNiCoAlO2 9% Co)	NCA	NCA	Gaining importance in electric powertrain and grid storage
Lithium Titanate	Li4Ti5O12	LTO	Li-titanate	

since a new and robust systems comes into our sight, Li-ion batteries. High capacity, high electrochemical potential, superior energy density, durability, and additionally the flexibility in design, make Li ion batteries more attractive. Li-ion batteries are now

increasingly used in portable electronic devices, 57.4% of sale on mobile phones, 31.5% on notebook computers, and 7.4% on digital cameras. Additionally their use has also been extended over other fields, including hybrid electric vehicles, space applications, military vehicles etc.The differences between various batteries are shown in Table 1.2

TABLE 1.2: The comparison between various batteries (Source: [9])

Cathode	Li-ion	Pb-Acid	Ni-Cd	Ni-MH
Lifetime/cycle	500∼ 1000	200 ∼ 500	500	500
Working Potential/V	3.6	1	1.2	1.2
Specific energy/Wh kg^{-1}	100	30	60	70
Specific energy/Wh L^{-1}	240	100	155	190

$LiCoO_2$ was first cathode material for Li ion batteris in 1990. Its long history supports $LiCoO_2$ a big development. After a while, other cathode materials have been identified, $LiNiO_2$, $LiMn_2O_4$, $LiNi_{1/3}Co_{1/3}Mn_{1/3}O_2$, $LiFePO_4$ et al. Comparisons of electrochemical parameters of numerous cathode materials are listed in Table 1.3

TABLE 1.3: Electrochemical parameters of several cathode materials (Source: [5])

cathode	$LiFePO_4$	$LiFePO_4$ +5%C	$LiMn_2O_4$	$LiCoO_2$	$LiNi_{0.8}Co_{0.2}O_2$
Density/g cm-3	3.60	3.48	4.31	5.10	4.85
Potential/V	3.50	3.50	4.05	3.90	3.6
Specific capacity /mAh g-1	169	159	148	274	274
Specific energy /Wh g-1	0.59	0.56	0.56	0.98	0.98

Each of them has their own characteristics. For example, $LiCoO_2$ is costly and toxic, and its resource is no longer plentiful [20]. $LiMn_2O_4$ enjoys a much lower capacity and inferior cycle stability [21]. Iron-based compounds look attractive as Fe is abundant, inexpensive, and less toxic than Co, Ni, or Mn. The phospho-olivine $LiFePO_4$ is currently under extensive studies due to its low cost, low toxicity, high thermal stability and high specific capacity of $170mAhg^{-1}$. Reduced reactivity with electrolytes brings about the very flat potentials throughout charge-discharge processes. The possibility of a material is partly decided by the Fermi level [22]. Much lower Fermi level is needed to accomplish a higher working voltage. Among the iron-based compound, particularly in$LiFePO_4, (PO_4)^{3-}$ brings down the Fe3+/Fe2+ redox energy to practical levels. Strong covalent bonding inside the polyanion (PO4)3- reduces the covalent bonding to the iron ion, which brings down the redox energy of iron ion. The Fe3+/Fe2+ redox energy is at 3.5 eV below the Fermi level of lithium in $LiFePO_4$. The lower is the Fe3+/Fe2+ redox energy

and the higher the V vs. lithium for that couple. In $LiFePO_4$, about 0.6 lithium atoms per formula unit can be extracted at a closed-circuit voltage of 3.5 V vs. lithium. The most noticeable advantages of $LiFePO_4$ are: (1) The structure of material hardly changes while Li ion intercalation and deintercalation and (2) It holds a prolonged voltage platform. The working principle of Li-ion battery is shown in Figure 1.4. Lithium ions move from anode to insert in cathode in the discharge process and reverse for charge process. $FePO_4$ is the second phase that is available on electrochemical extraction of lithium from $LiFePO_4$. The extraction of lithium from $LiFePO_4$ to charge the cathode may be written as Formula 1 and the insertion of lithium into $FePO_4$on discharge as formula 2. "X" in the folowwing formulas is the number of electrons that are being exchange between anode and cathode during charge and discharge processes.

1. LiFePO4 - xLi - xe- →xFePO4 + (1 - x)LiFePO4
2. FePO4 + xLi+ xe- → xLiFePO4 + (1 - x)FePO4

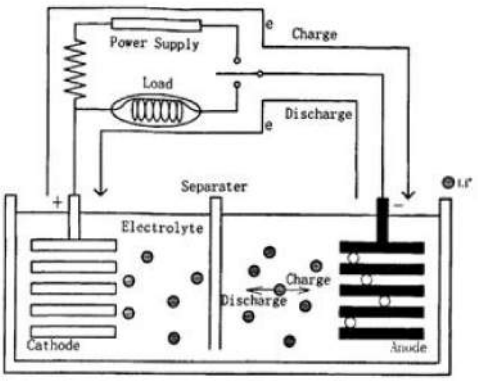

FIGURE 1.4: The schematic diagram of working principle for lithium battery (Source: [5])

More researches are being conducted for Li ion batteries specially for lithium ion phosphate as cathode materials in order to invent a composite cathode of iron and transition metal oxides like $LiCoO_2, LiNiO_2$) [5].

1.6 Battery Based Stand-alone PV Systems

Stand-alone PV systems need battery to save enough energy for periods without enough adequate solar radiation. Unfortunately battery in stand alone systems is the weakest

point of the system. Therefore 30% or even more of lifetime expenses of solar off-grid systems goes to storage. Frequently, the storage battery of a stand-alone PV system is sized to guarantee, if the solar irradiation is inadequate, the imagined loads could be powered for at least 3 to 4 days. The product of such typical sizing is that the daily depth of a PV battery discharge is in the range of 25 to 30% of its rated (10 h) capacity. Besides, the dimensioning of the PV generator might generally be expected to cover the entire energy request of the foreseen loads under normal sun conditions. These two fundamental assumptions allow the following points with respect to the typical operating conditions of a battery in a stand-alone PV system to be presumed (see also Figure 1.5):

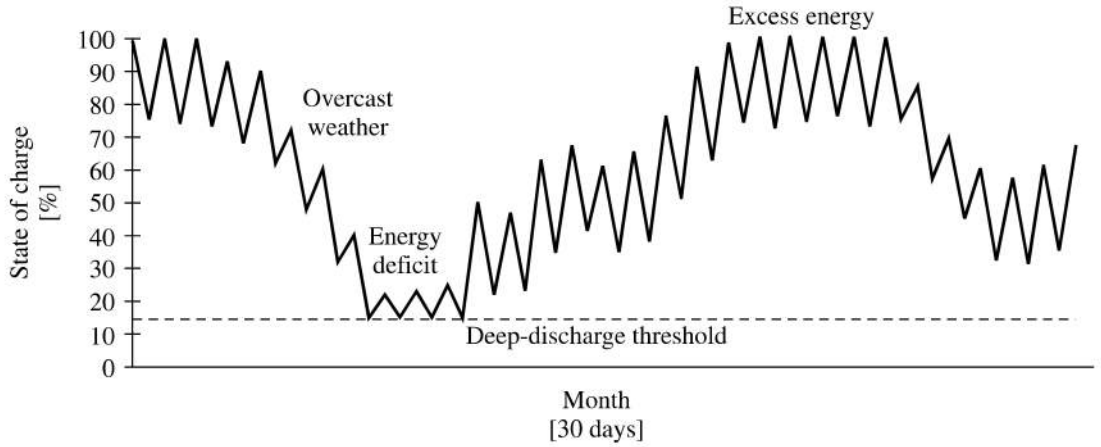

FIGURE 1.5: Operating conditions of batteries in PV systems (Source: [6])

Consequently, the operating conditions and lifetime of a PV battery are basically estimated by the number of days when the battery realizes 100% full charge condition (which is the ideal) and the number of days when it achieves the minimum discharge voltage threshold (worst operating condition). Assuming the PV generator has been sized to be extremely small for the predicted loads, the battery will reach deep discharge conditions more often throughout the year and its lifetime will be short. Provided that, instead, the PV generator is over-dimensioned, the battery will achieve 100% full charge conditions about every day of the year, and it will have longer lifetime [7]. As battery lifetime is one of the important considerations determining lifetime expenses of the entire stand-alone Photovoltaic system, LiFePO4 battery is considered for this investigation. Due to the noticeably decreasing expenses for solar panels in the last few years, batteries are playing, cost wise, a more principal role. Their limited lifespan in comparison with solar modules (20+ years) raises the total cost of the entire system respectively.

Since lead acid batteries have several disadvantages like possible acid leakage, poisonous vapor given during charging and their extra weight, they are not attractive for stand alone systems anymore. Also disposal of lead acid batteries can cause environmental problem which leads to health risk for people's lives in long time. In addition to all the mentioned issues, these batteries has againg problem when they kept in low state of charge. All these leads cost over time.

However, LiFePO4 batteries are widely utilized within electrical mobility applications, because of their preferences over different sorts of battery types: one of its significant characteristics is the superior thermal and chemical stability, which delivers preferable safety properties over lithium-ion batteries with other cathode materials. Because of stronger bonds between the oxygen atoms in the phosphate (contrasted with cobalt, for instance), oxygen is not easily discharged and as a result, lithium iron phosphate cells are nearly incombustible in the occasion of misuse, and can survive high temperatures up to 85C without decomposing. The LiFePO4 battery is friendly to the environment, there is no dangerous or harmful substance inside the battery, which is also a superb characteristic for stand-alone solar system application, on the grounds that the greater part of the end users are located in remote zones, where safety awareness is extremely low. The specific volume and the weight of a LiFePO4 battery is 65% and 33% of lead-acid batteries respectively, which also makes the battery more portable. The total lifespan (cycles) is around 2000 cycles with the limit as of now arriving at 80%, which is 6-7 times higher than lead acid batteries over the whole lifetime. Additionally, it is maintenance-free and does not get influenced by more extended lengths of time in low states of charge, which allows a higher use of its ability [6].

Chapter 2

Rationale for Study

In this section the main goals are: concentrating on the study justification, describing the problem, and explaining the final goal of the investigation.

2.1 Motivation

In developing countries such as Turkey a small solar panel and a battery to run a few lights and a radio can change peoples' lives. There are several faraway and remote areas in this country where people do not have a sufficient access to electricity. Also there are so many agricultural areas in this country and countries similar that in summer season they need continuous electricity support for irrigation. However, always the lack of a well-developed system has been known especially in some rural areas, an energy provision can affect many consumers. Also application of renewable energy sources can be more effective for far and remote areas. For example, in case of coal-fired energy source there are several problems. First of all coal transportation has cost. Second, it is not a safe system. Besides, it cause carbon dioxide emission while leads to health risk for human kind and it is not environmentallly friendly. In addition to all of these, in sever and harsh climate coal delivery may have delay as well. However, in case of solar energy, the transportation is free since the sunlight is every where, and it is maintnance free for long years. also it is safe and environmentally friendly. Because of this, an energy providing system such as a solar panel and a battery can effect on so many aspects of these sorts of consumers.

2.2 Problem Statement

Turkey is a poor country in terms of oil, natural gas and coal. The country is already paying a large amount of money for providing energy to countries like Iran, Russia, Kazakhastan, Iraq, and Saudi Arabia. On the other hand, it is located in a proper geographic area from solar irradiation aspect.

The mentioned energy issue was an initial motivator for running this project. In the first step, a high efficiency silicon solar cells with a hetro-junction microcrystalline intrinsic thin layer (HIT) was investigated as a PV material. An efficiency of 24.5% for the proposed structure was reported [23]. Detail results of this research is mentioned in chapter 3. However, since the proposed PV material was not avaliable, a simple a-Si material which is avaliable in the market was considered for the PV system of this research. In the next step, a storage system was described for the PV system in order to have a stand alone photovoltaic system. A cheap, light and mobile system was the main objective of the project. These three options, made lithium ion batteries the best possible choice. Lithium Iron Phosphate (LiFePO4) battery was choosen among Li ion batteries in order to assemble the BSPV system. Meanwhile solar irradiation and temperature data was collected for Istanbul, Ankara and Adana with different climates [24]. In this stage of work all the modules necessary data for designing a BSPV was ready. Therefore, by appliying proper formulas and theories a BSPV with eight series of LiFePO4 batteries and three a-Si panels with efficiency of 7% was desigened. Further information about the the modules are discussed in the next chapters.

2.3 Justification of the Study

Turkey is in the process of fast industrialisation, while the population also increasing rapidly. This means the country energy requirment is increasing with a high acceleration rate. Currently Turkey is almost dependent to fossil fuels such as oil, coal and natural gas in order to meet its energy demands. Apparently becasue of lack of fossil fuel resources and global climate and environmental problems developing countries like Turkey should set a promising schedule for using renewable energy sources like photovoltaic materials. Oil is the main and primary energy source with demand of 40.9%. However, this percentage is decreasing as the consumption of natural gas is increasing and it is expected to

Table 2.1: Solar technologies barriers in Turkey

General Obstacles for Solar Technologies in Turkey
Economical disadvantages
Govermental barriers problems with research on solar energy
Intermittent energy
Public unawareness about solar technologies
Reluctance of people to change
Lack of information flow/communication networks
Aesthetics
Lack of democracy
Polluting technology imposed on deveoping countries
Technology is not ready yet, the efficiency is low
Fossil fuel companies has lobbies against PV

decrease to 24% by 2020. Nearly 90% of Turkey's oil supplies are imported from Middle East and Russia. Therefore if country wants to get ride of forigen countries dependency it should go toward renewable energy resources. Here are the general obstacles seen by scientists, NGO's and experts for solar technologies for Turkey 2.1.

These were the main barriers toward solar technologies specially about photovoltaics. However, these issues look as already solved problem with first world countries like USA and Canada. It is true that there are so much to do in developing countries like Turkey in order to tackle the barrires. However, it looks year by year production of energy from renewable resources specially PV is rapidly increasing [25]. From a technical point of view, it is imperative to analyze the performance of a BSPVS because the results of the analysis form the basis of improving the systems.

2.3.1 The application of BSPV in the world and Turkey

BSPV systems has several applications in off-grid power supply systems. In a general division off-grid power supply can be divided into three subsections as Consumer applications, Industrial applications and Remote habitation. Figure 2.1 shows each categories applications. Renewable energy specially solar energy is under investigation. The total installed capacity of solar panels is estimatated as much as 1000MW by 2014 [26]. By considering the good potential of the country a mobile, light and cheap BSPV system is designed in order to be used in off-grid applications.

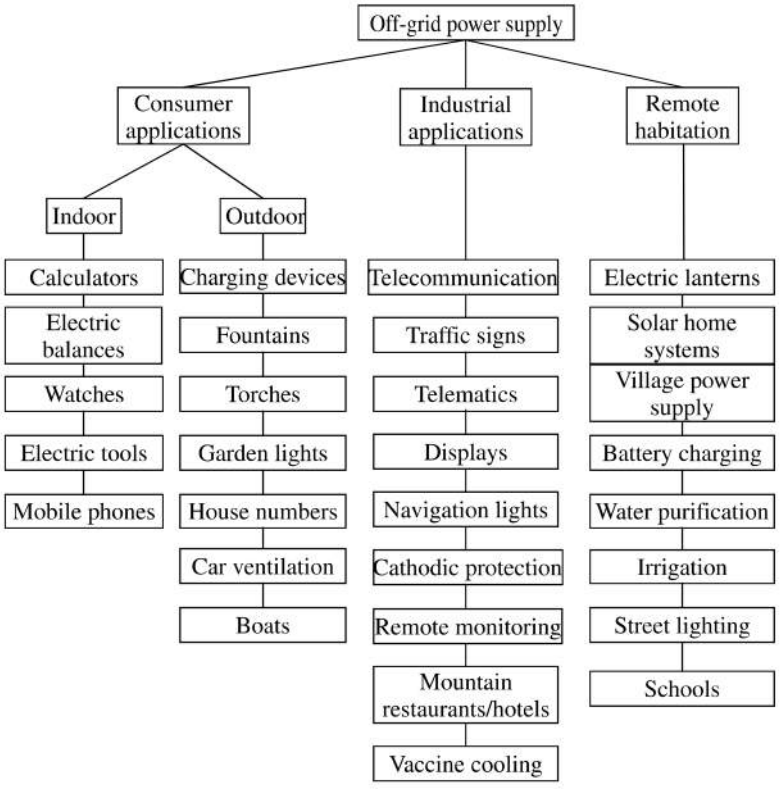

FIGURE 2.1: Application areas of BSPV (source: [7])

2.4 Goal and Scope of the Study

Solar energy is the most important alternative clean energy resource in Turkey. The yearly average solar radiation is $1,311 kWh/m^2$ per year and $3.6 kWh/m^2$ per day. The total yearly insulation period is approximately 2,460 hours per year and 7.2 hours per day. The solar power in Turkey as it can be seen in Figure 2.2 is located in an advantageous position in Europe for the purposes of solar power. Compared to the rest of Europe, insolation values are higher and conditions for solar power generation are comparable to Spain [27]. This annual solar radiation provides an annual energy potential of about 1,512 TWh. However, according to technical report [26] "Turkey's teachnically feasiable electricity potential from wind power plants ranges between 200 and 400 TWh. While, the econimically feasible potential lies between 35-70 TWh." In order to analyze a BSPV system in Turkey three cities with different climates and solar radiation are considered. Istanbul, Ankara, and Adana were investigated in terms of temperature and solar radiation. The effect of environment temperature on the silicon panels is considered. Since a battery is a critical part of a BSPV system, a battery simulator is used in order to

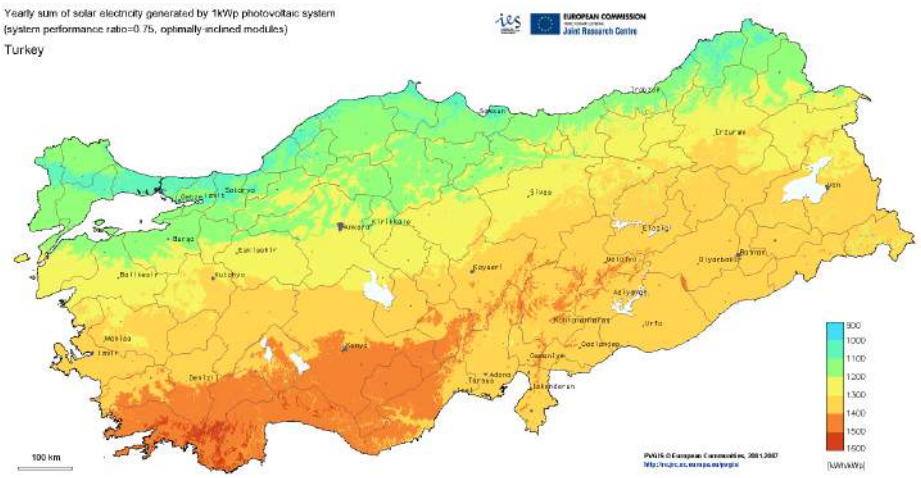

FIGURE 2.2: Turkey solar map

analyze the balance of the system. The main goal of the project is to design a system that is mobile, light, and cheap. That is why amorphous silicon has been considered as the photovoltaic material in order to keep the price of the system as low as possible. Also for keeping the system light enough to be able to move easily LiFePO4 batteries has been used. The results will be discussed in the following chapters.

Chapter 3

Theory and Calculations

In this chapter, different aspects of a high efficiency silicon solar cell and a simple a-Si for electricity generator module is discussed. In the second step, it is shown how to apply solar irradiation and temperature data into relevant formulas in order to calculate amount of deliverable power and energy values by applied panels. In next steps, applied Li Iron Phosphate battery and set up for running the tests are explained.

3.1 High Efficiency Silicon Solar Cells with a Hetero-junction Microcrystalline Intrinsic Thin Layer

A high efficiency silicon solar cells with a hetro-junction microcrystalline intrinsic thin layer was investigated. The influence of different parameters such as the temperature, the back surface field, different layer thicknesses, different doping concentrations for p and n type layers, ZnO and ITO as (TCO) transparent conductive oxides with plane and texturized surface shapes and densities of interface defects (Dit) on the efficiency was investigated. For simulation of hetero-structures, AFORS-HET software was used in the study. Our results indicate that by optimizing different parameters of hetero-structure thin films, a high performance can be obtained using nanostructured surfaces up to an efficiency of 25% for HIT silicon solar cells [28]. Figure 3.1 shows a schematic structure of simulated silicon solar cell. Some of the simulation parameters, such as a-Si:H layers, and the c-Si(p) base are the default values in the AFORS-HET software that can be found in Table 3.1.

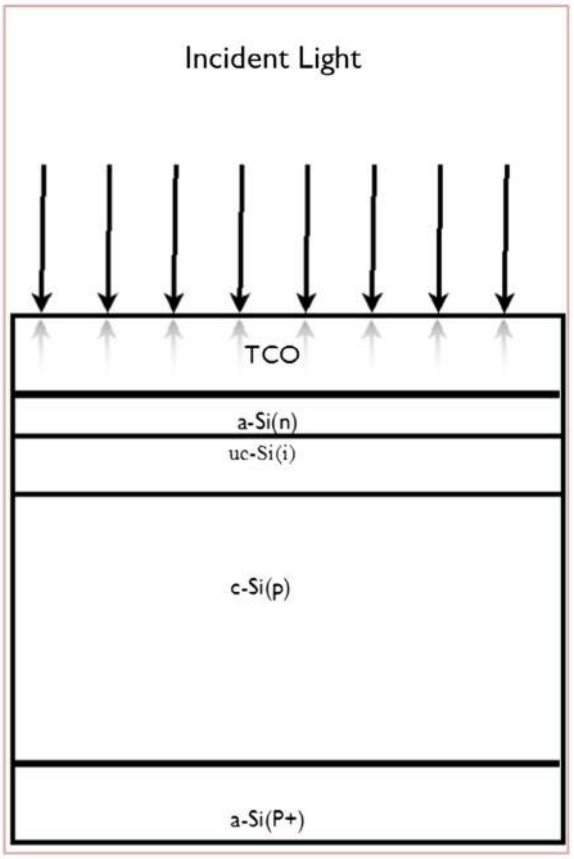

FIGURE 3.1: Schematic basic structure of simulated solar cell TCO/a-Si:H(n)/μc-Si:H(i)/c-Si(p)/ a-Si:H(p+)

3.1.1 Optimization of Emitter Layer

Simulation results are showing that as the thickness is reduced, the current becomes higher. However, there is difficulty in practice manufacturing a repeatable thickness value less than 3 nm, therefore the most realistic thickness is 3 nm. Using this thickness, an excellent efficiency can be obtained by the solar cell. Figure 3.2 shows the effect of thickness of this emitter layer on current.

3.1.2 Optimization of the Intrinsic Layer

While there is argument about the need of such a layer between p and n type doped layers for HIT [29] a μc-Si:H intrinsic layer was added to the proposed structure and the effect of its thickness on external current was investigated. Figure 3.3 is showing the obtained results. The reason of adding this layer is that density of states in undoped

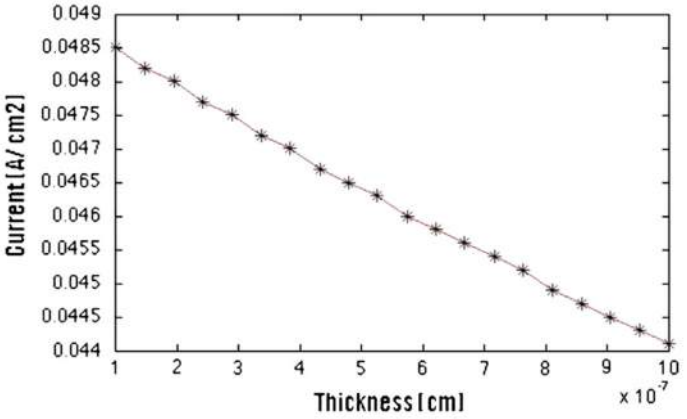

FIGURE 3.2: The dependence of external current of the structure as a function of the thickness of emitter

μc-Si:H is weaker than in doped a-Si:H. Therefore, when heterointerface is formed, there might have less interface defects.

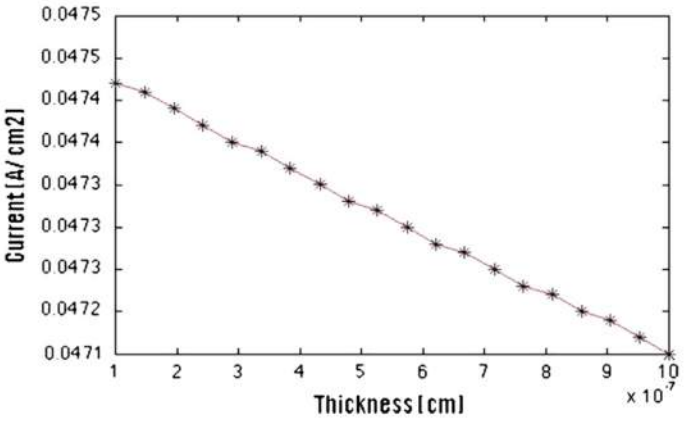

FIGURE 3.3: The dependence of external current of the structure as a function of the thickness of intrinsic layer

Figure 3.3 exhibits the effect of thickness of this layer on the solar cell external current, for a range of 3-10 nm. Solar cell external current reduces and by considering this fact that the current amount has direct impact on the final efficiency, therefore the efficiency will decrease. Also dependency of V_{oc} is so less to defect density or thickness of intrinsic layer and it is controled by simple physics of the spitting of quasi-Fermi levels in the intrinsic layer. According to Figure 3.4, the voltage is decreased by increasing the thickness of the intrinsic layer. As it can be seen in reference [30] this simulation result is in good agreement with the experimental data.

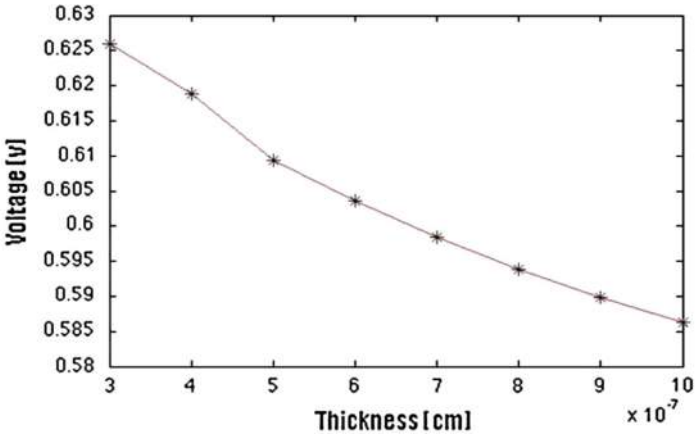

FIGURE 3.4: The dependence of Voltage on the thickness of intrinsic layer

3.1.3 The Influence of TCO on the Effeciency of the Solar Cell

Since the emitter and intrinsic layers are so thin, the impact of TCO is necessary to be investigated. Figure 3.5 shows texturized front surface of TCO in a schematic view. The application of highly conductive transparent layer is to transfer carriers to the metal contact. Radiation for texturazied standard Si $\langle 111 \rangle$ surface was simulated by AFORS-HET software. Final efficiencyiy for ITO and ZnO for texturized and planar surfaces are shown in Figure 3.6.

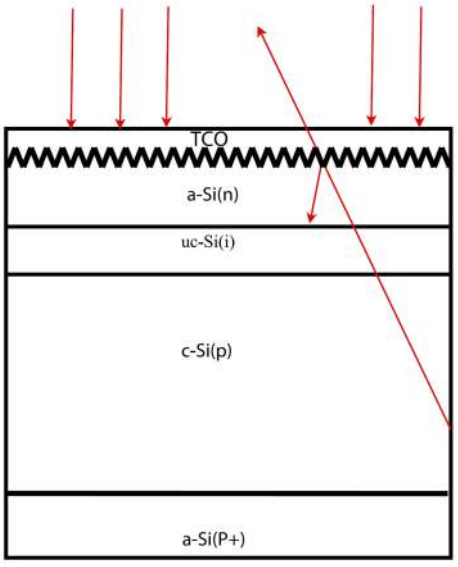

FIGURE 3.5: Schematic view of the textured TCO and the concept of light trapping due to scattering from this layer are depicted above.

As shown in Figure 3.6, the highest efficiency is for ZnO with a texturized surface solar cell with 24.5% and a planar structure with 23.33% efficiency and for ITO texturized and planar surface structured layers, the efficiency is 22% and 20.99%, respectively. Table 3.2 is giving the necessary information about the fill factor (FF), open-circuit voltage (V_{oc}), short-circuit current (J_{sc}) and efficiency (η) for each of the mentioned cells in the Figure 3.6.

Efficinecy of the cell is shown by the equation 3.1:

$$\eta = J_{sc} V_{oc} FF / P_s \tag{3.1}$$

P_s is incident light power in the above equation.

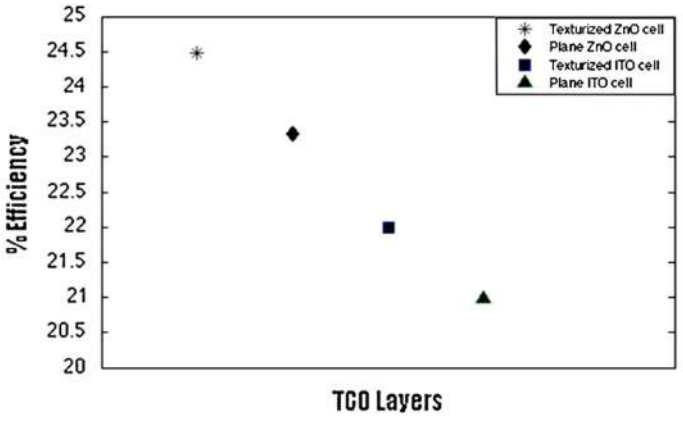

FIGURE 3.6: Different transparent conductive oxide layers and their efficiencies

3.1.4 The Effect of Defects in c-Si(p) Layer on the Efficiency

By increasing the interface defects density, reverse saturation current increase, open circuit voltage and fill factor decrease because of the increase in carrier recombination probability. All this make efficiency decrease. It is possible to control interface state defect density down to $10^{10} cm^{-2} V^{-1}$ by surface passivation method like plasma assisted H passivation. Figure 3.7 exhibits the influence of interface state defect density on the efficiency.

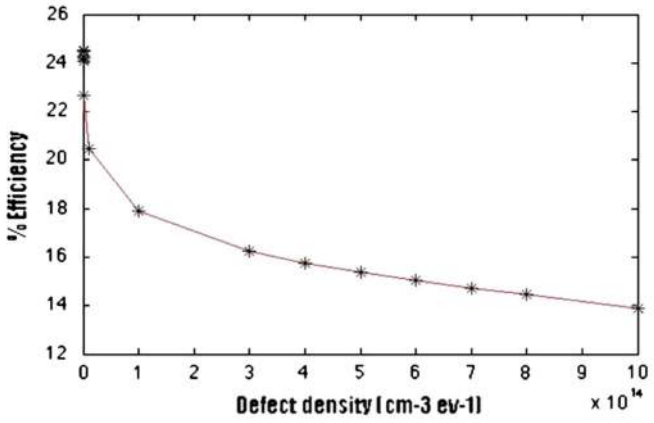

FIGURE 3.7: Impact of interface defect density in c-si(p) on solar cell efficiency

3.1.5 The Effect of a-Si(p+) BSF Doping Concentration on the Device Efficiency

Figure 3.8 shows the influence of BSF doping concentration on the photovoltaic characteristics of solar cell. In this graph, we can see that the doping concentration must reach a certain value, preferably more than 10^{20} cm^3 to observe good conversion efficiency. Because of the BSF band structure, increasment in doping concentration the open circuit voltage,short circuit current and fill factor increase as well. Unclear reflection role of BSF while the doping concentration is low and barrier reduction of carrier transport by increasing the doping concentration are two reasons that explain why high doping concentration BSF is a guarantee of good BSF.

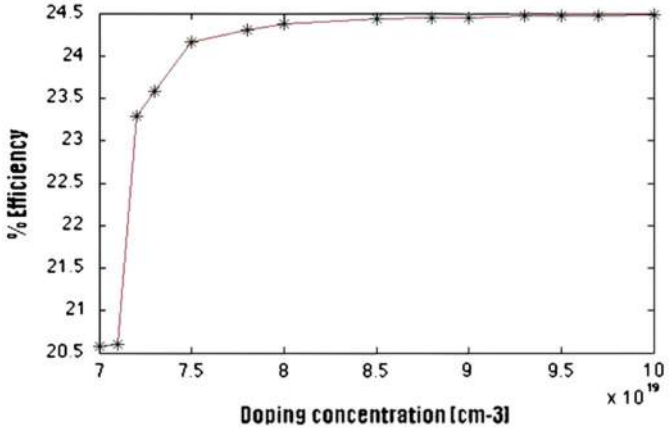

FIGURE 3.8: Dependency of efficiency to BSF doping concentration

3.1.6 The Effect of BSF Thickness

Figure 3.9 exhibits the effect of the BSF thickness on the efficiency characteristics of HIT solar cell. As it can be seen the efficiency can be considered almost unchanged. This result is production time saving and cost effective since the lowest possible manufacturable BSF can be appropriate for this structure. Therefore, the BSF thickness can be set to 5 nm.

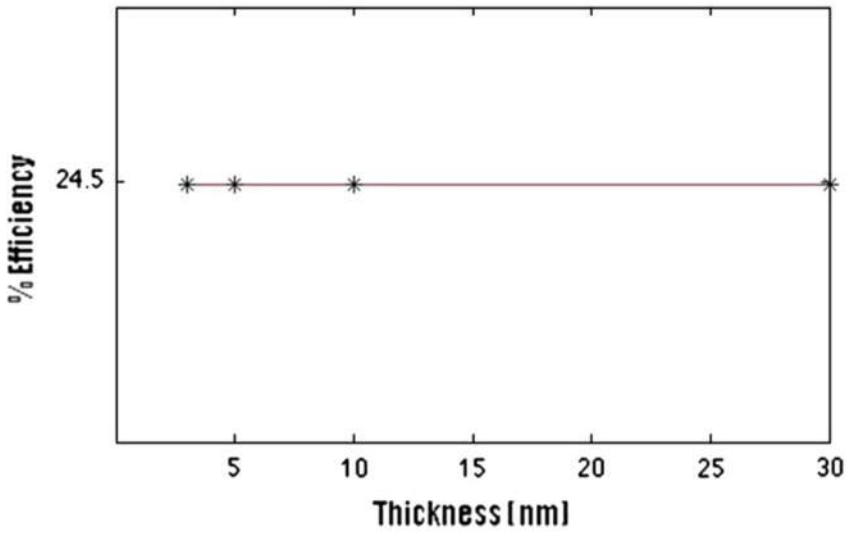

FIGURE 3.9: The effect of thickness on the efficiency is shown

3.1.7 The Effect of Temperature on the Efficiency

One of the important factors of solar cell efficiency is the temperature. In this investigation, the impact of temperature was considered on the mentioned HIT solar cell structure. As it can be seen in Figure 4.14, the efficiency will decrease gradually as the temperature is raised from 300 K to 343 K.

Increasing temperature mostly affect open circuit voltage. Since the number of electrons n_i increases exponentially, by increasing temperature, dark saturation current density (I_0) increases. It is necessary to mention diffusion component of the dark current effect beats the recombination-generation, because of stronger dependence on n_i (Eqs.3.2 and 3.4) . The increased dark current reduces Voc according to the Eq. 3.5 . Meanwhile bandgap reduced and photocurrent increased since lower energy photons can be absobed by increasment of temperature. The net effect is a reduction in the efficiency becasue the loss in V_{oc} outweights the gain in J_{sc} [8].

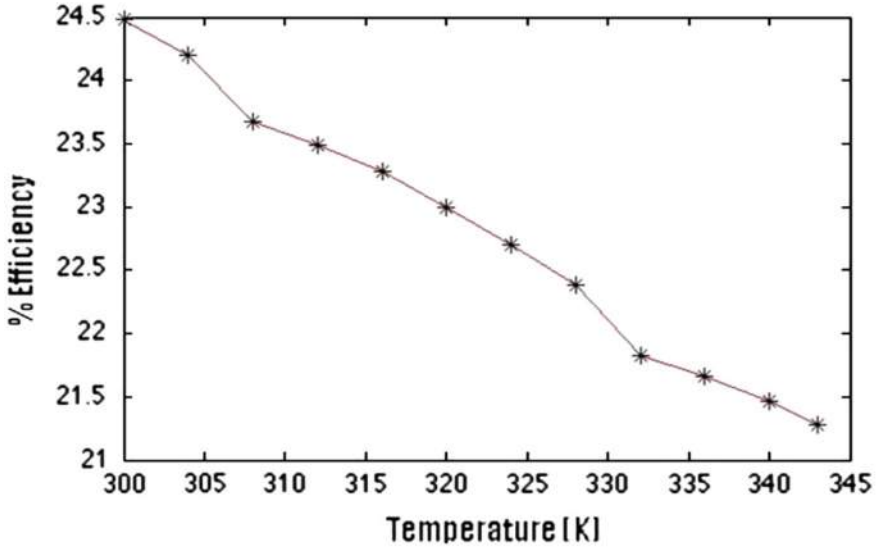

FIGURE 3.10: The effect of temperature on the efficiency is shown

$$I_0 = qADn_i{}^2 / LN_0 \tag{3.2}$$

where q is the electronic charge, D is the diffusivity of majority carrier, L is the diffusion length of the minority carrier, N_0 is doping and n_i is the intrinsic carrier concentration.

$$n_i{}^2 = 4(2\pi kT/h^2)^3(m_e m_h)^{3/2} \approx BT^3 \exp(-E_{G_0}/KT) \tag{3.3}$$

where T is the temperature, h and k are constants,m_e and m_h are the effective masses of electrons and holes respectively. E_{G_0} is the band gap linearly extrapolated to absolute zero and B is a constant which is essentially independent of temperature.

Substituting equation 3.3 to equation 3.2 gives following equation:

$$I_0 = qAD/LN_0\dot{B}T^g \exp(-E_{G_0}/KT) \tag{3.4}$$

where $\dot{B}$ is a temperature independent constant. A constant, g is used instead of the number 3 to incorporate the possible temperature dependencies of the other material parameters.

On the other hand, V_{oc} and I_0 are dependent according to the following equation:

$$V_{oc} = \frac{KT}{Q} \ln(\frac{I_{sc}}{I_0}) \tag{3.5}$$

where I_{sc} is the short-circuit current. The impact of increasing temperature is shown in the Figure 3.11. Also Our simulation results show good correlation to the experimental results from [31].

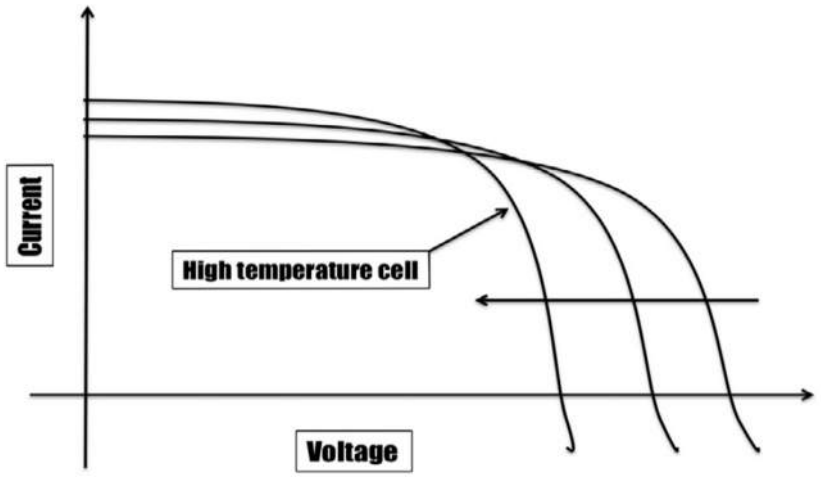

FIGURE 3.11: Effect of temperature on p-n junction J(V) characteristic. The arrow indicates the direction of increasing intensity or temperature [8]

3.2 Applied Silicon Solar Cell Material

In this investigation, in order to design a battery based stand-alone system three parallel a-Si panels are used as the electricity generator since HIT silicon solar panel was not avaliable. Silicon is being used in simiconductor industry for several years. Also solar cell industry has started to use this material since the first days. There are several reasons for this but the first is that simply it is easy to make silicon devices. This means that althought silicon is not the best material for solar cells, because of this reason, availablity and low cost of this material it could book a major part of solar cell market. What makes silicon devices easy to make is a unique oxide layer that forms on its surface when heated to high temperatures which remove defects on the silicon surface and it allows back to back easy processing [28].

FIGURE 3.12: An applied a-Si panel in this study

The provided electricity is tranported to LIF battery package. This system is evaluated in this study in terms of voltage, energy, and capacity for each month in a complete year for three cities of Istanbul, Ankara, and Adana. Properties of Panels are in the Table 3.3. The reason that a-Si panel is chosen is that it is the cheapest and the most available material in the industry also it has high durability and it is almost maintenance free. Figure 3.12 shows an applied sample panel of a-Si.

3.3 Solar Irradiation Data of Istanbul, Adana, and Ankara

In this study, three different cities Adana, Ankara and Istanbul were considered in order to measure the temperature and radiation effects of these cities on the performance of the panels. These measurements direct the study to have a realistic estimate for panel's output. Table 3.4 shows the solar radiation in Istanbul, Ankara and Adana.

Temperature data are extracted from the Figures 3.13, 3.14 and 3.15 [24]. As it can be seen there are two curve in each graph which are showing Min and Max avaerage temperature for each month. In order to have a balance set of temperature data, average was taken from two sets of temperature data provided in the temperature graphs. The average of these two trends gives a third line between them which is the temperature data that is applied for this research. The average temperature summary is written in the Table 3.5.

3.4 The Formulas for Theoretical PV Calculations

The photovoltaic's (PV) manufacturers normally rate the modules base on the standard test condition (STC) that is 25∘C, 1000 W/m^2 and 1.5 G of air mass, whereas each

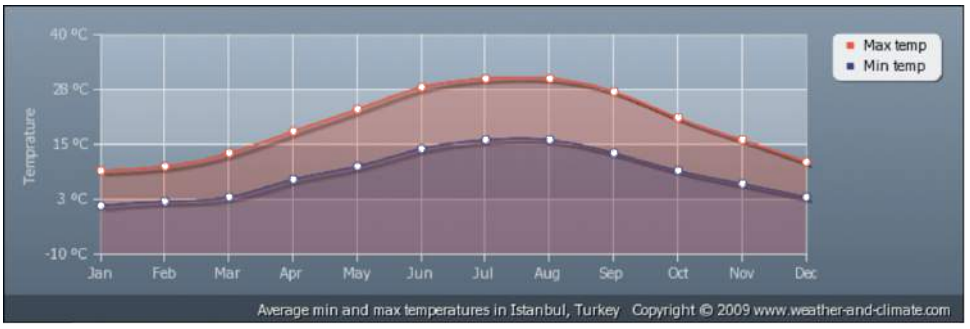

FIGURE 3.13: Max and min Temperature of Istanbul

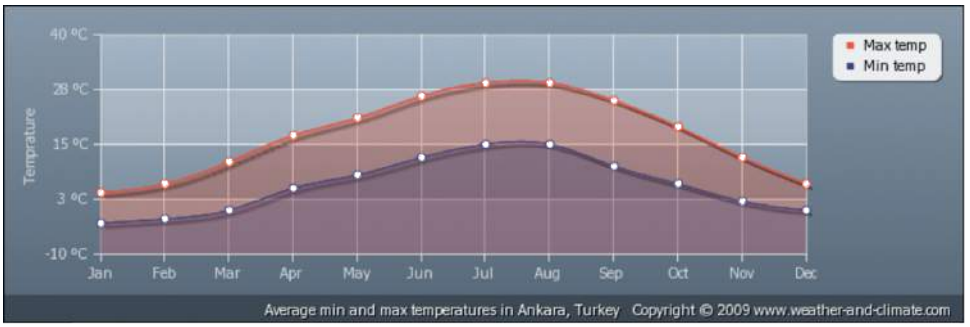

FIGURE 3.14: Max and min temperature of Ankara

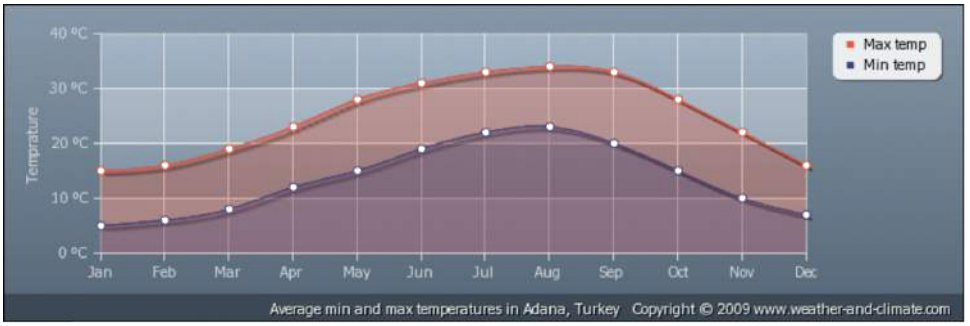

FIGURE 3.15: Max and min temperature of Adana

module might operate under different environmental conditions that have various temperature, irradiance and sunlight spectra. As a result the PV industry needs to enhance the power rating approach by introducing new standards and more comprehensive rating methods. For example there might be a PV cell that is designed to work in the standard conditions, but it is being used in Istanbul with different environment circumstances and latitude. In this case the efficiency that is reported by company won't be realistic and it even may have result faraway with what might be anticipated. In order to have more precise estimate following formulas and calculations are applied.

The International Electrotechnical Commission is a "non-profit, non-governmental international standards organization that prepares and publishes International Standards for all electrical, electronic and related technologies" as well as photovoltaic industry [1]. The IEC 60891 and NREL provide four procedures to translate and correct measured Current-Voltage characteristics to the standard test condition or any other selected temperatures and irradiances [32].

Since radiation and environment temperature affect the efficiency of solar modules and manufacturers are giving the data according the STC standards it is necessary to know what will be current and voltage according to our temperature and radiation conditions. But first it is necessary to calculate the temperature of the module while it is working. For variations in ambient temperature and irradiance the cell temperature (in ∘C) can be estimated accurately with the linear approximation of Luque and Hegedus as follow:

$$T_c = T_a + \frac{(T_{NOCT} - 20)}{(0.8KW/m^2)} * I(t) \tag{3.6}$$

Here T_a is ambient temperature and T_c is cell temperature. The NOCT (Nominal Operating Cell Temperature) value in the equation varies between 42 ∘C and 46 ∘C for today's PV modules. As a result the C(t) value varies between 0.0272 until $0.0321 \circ C/(W/m^2)$.

$$C(t) = (T_{NOCT} - 20)/800 \tag{3.7}$$

for this study the highest possible amount is considered for this panel, which is 0.0321 ∘C/(W/m^2). Therefore following translation equations are used:

$$I_2 = I_1 + I_{SC}[G_2/G_1 - 1] + \alpha(T_2 - T_1) \tag{3.8}$$

$$V_2 = V_1 - R_s.(I_2 - I_1) - k.I_2.(T_2 - T_1) + \beta.(T_2 - T_1) \tag{3.9}$$

Table 3.6 defines different parameters in equations 3.8 and 3.9.

By inserting data from Table 3.5 into Equation 3.6 panels temperature in different months is calculated. Also, by using Tables 3.5 and 3.3 data and applying Equation 3.8 panels current is obtained. Tables 3.7, 3.8, and 3.9 show panel's temperature, current and max voltage per month in sequence of one year respectively.

Therefore according to the above tables it is possible to calculate power values from a simple multiplication of voltage to current values for each panel for each month. Table 3.10 exhibits the power values for each month for the mentioned cities.

As it is mentioned Turkey has 7.2h average effective sunshine per day. By multiplying time value with the power values, the energy values that are produced per day are calculated. Table 3.11 shows the calculated energy values per month.

All these calculations are done for one panel, however the designed system has three of these panels. Therefore, all the values values will be multiplied accordingly. Therefore, the results for the three panel systems will be introduced in the next chapter.

3.5 Li Iron Phosphate Batteries

For the electricity storage part high power LiFePO4 batteries were applied. The specifications of this type of battery cells are sorted in Table 3.12.

Each package of battery contained five parallel cells. Therefore, it is possible to get a current between 13 to 15 Ah from each battery package. As eight packages of these batteries were used the following calculations make sense.

- Max necessary voltage for charging the system is $8 \times 3.65 = 29.2$V
- Minimum necessary voltage is $8 \times 2.75 = 22$V
- Nominal voltage for charging the battery system: $8 \times 3.2 = 25.6$ V

Consequently, the system might be able to store $25.6\text{v} \times 13\text{Ah} = 360\text{Wh}$ energy . The battery simulator results in conjunction with solar panels will be discussed in the following chapter.

3.6 Battery Cycler

Digatron Firing Circuits is the commercial name of the software that was used in order to program the solar insulation.

This system is for energy storage and testing, which is designed for today's requirements of a state of the art battery test system. It is a computer controlled test system. Today's battery development is focused on future battery systems like Li-ion batteries. These batteries will power electric vehicles, UPS-Systems (uninterruptible power supply) and portable electronic equipment. The procedures for this generation of batteries are much more expensive and sophisticated than those for SLI batteries (starting, lighting, ignition). The test methods are much more related to the construction and application of the battery. Simulation of final application is of growing importance. It is not acceptable a battery endures 1200 IEC/SAE cycles without any problem only to fail in the practical use after only one year of operation. Application orientated test procedures demand unrestricted flexibility from a test system. BTS (Battery test system) has several key features like program library with ultimate number of test programs, total flexibility to structure the entire program schedule, highly flexible program schedule with no prefixed fill-in requirements, all wordings are in battery terms or may be customized, sampling rate can be based on the same features as limit conditions and cycles may be terminated by a preset number or by any other system parameter [33]. Figure 3.16 shows a sample interface of the software.

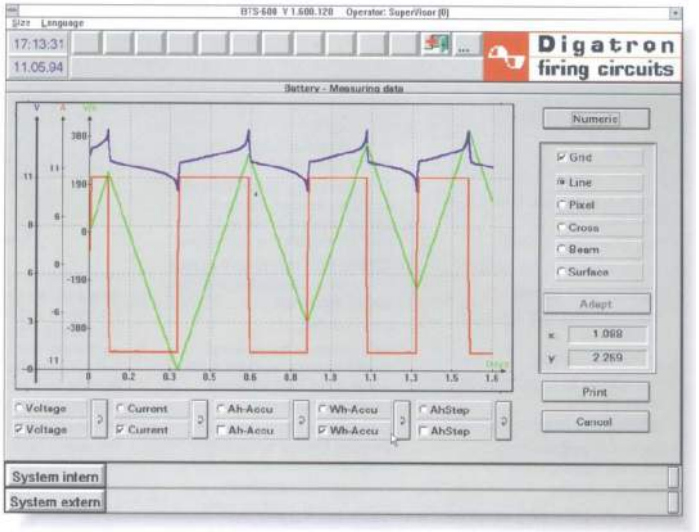

FIGURE 3.16: Digatron firing circuits software interface

3.6.1 Universal Battery Tester

The Universal Battery Tester (UBT) is particularly designed for life cycle and capacity testing of automotive batteries. It can also be used for testing other types of batteries. The UBT performs charging and discharging in accordance with the programmed test schedule. Parameters are constant current, constant voltage, constant resistance and constant power. For data evaluation, the UBT runs either with Digatron/Firing Circuits well-known Battery Manager or BTS-600 software. Battery Manager is usually applied for quality assurance and high volume testing, whereas BTS-600 is used for research and development requirements. In the standard version, one cabinet contains 5 or 10 charge-/discharge circuits connected to one common DC bus bar power supply. Numerous options are available such as paralleling circuits, single cell operation, cell/battery drop out, multi range switching, temperature inputs, inputs for reference electrodes, data-logger interface, CAN-Bus interface as well as digital inputs and outputs and a RS 232 interface to the climatic chamber [33]. Figure 3.17 shows the UBT.

FIGURE 3.17: A Universal battery tester

TABLE 3.1: Some initial parameter values adopted for the HIT solar cells in the investigation

Parameters	**a-Si:H(n)**	**μc-Si:H(i)**	**c-Si(p)**	**a-Si:H(p)**
Layer thickness (nm)	3-10	3-10	$4 \times 10_5$	5-30
Dielectric constant	11.9	11.9	11.9	11.9
Electron affinity (eV)	3.9	4	4.05	3.9
Band gap (eV)	1.72	1.2	1.124	1.72
Optical band gap (eV)	1.72	1.4	1.124	1.72
Effective conduction band density (cm^{-3})	1×10^{20}	3×10^{19}	2.8×10^{19}	1×10^{20}
Effective valance density (cm^{-3})	1×10^{20}	2×10^{19}	1.04×10^{19}	1×10^{20}
Electron mobility ($cm^2V^{-1}S^{-1}$)	5	50	1041	5
Hole mobility ($cm^2V^{-1}S^{-1}$)	1	5	412.9	1
Doping concentration of acceptors (cm^{-3})	0	0	1.5×10^{17}	1×10^{20}
Doping concentration of donors (cm^{-3})	6×10^{18}	0	0	0
Thermal velocity of electrons (cms^{-1})	1×10^{07}	1×10^{07}	1×10^{07}	1×10^{07}
Thermal velocity of holes (cms^{-1})	1×10^{07}	1×10^{07}	1×10^{07}	1×10^{07}
Layer density (gcm^{-3})	2.328	2.328	2.328	2.328
Auger recombination coefficient for electron (cm^6s^{-1})	0	0	0	0
Auger recombination coefficient for hole (cm^6s^{-1})	0	0	0	0
Direct band to band recombination coefficient (cm^3s^{-1})	0	0	0	0

TABLE 3.2: The fill factor, open circuit voltage, short circuit current and the efficiency of each cell

$Parameter/cell$	V_{oc} (mV)	J_{sc} (mA/cm^2)	$FF\%$	$E_{ff}\%$
Texturized ZnO	626	47.4	82.49	24.48
Plane ZnO	624.9	45.28	82.46	23.33
Texturized ITO	623.1	42.84	82.4	22
Plane ITO	622	40.98	82.35	20.99

TABLE 3.3: A-Si panel properties

Maximum power (Wp)	20W
Maximum power voltage (V)	23
Maximum power current (A)	0.86
Open circuit voltage (V)	30
Short circuit current (A)	1.03
Size of module (mm)	1250*323*25
P-I-N Junction	double junction
Maximum system voltage (V)	1000V
Temperature coefficients of Isc (%)	+0.09/∘C
Temperature coefficients of Voc (%)	-0.33/∘C
Temperature coefficients of Pm (%)	-0.22/∘C
Temperature Range	-40Â°C to +85∘C
Weight per piece (kg)	9.5
Junction Box	Waterproof, TUV certificated
Cell Efficiency (%)	7%
Watt tolerance(%)	± 3%
Encapsulant	EVA(Ethylene Vinyl Acetate)
Frame (Material, Corners, etc.)	Anodized Aluminum Alloy
Front glass	3.2mm annealed glass
Back side	Float Glass
Frame (Material, Corners, etc.)	frame
Standard Test Conditions	AM1.5 $100MW/cm^2$ 25∘C
Warranty	90% power for 10years, 80% power for 20 years.

Table 3.4: Solar radiation in Istanbul, Ankara, and Adana [10]

Solar Radiation/ Month	Average Solar Radiation Istanbul (W/m^2)	Average Solar Radiation Ankara (W/m^2)	Average Solar Radiation Adana (W/m^2)
January	192.90	289.35	308.64
February	385.80	462.96	482.25
March	540.12	617.28	636.57
April	694.44	752.31	771.60
May	810.18	848.77	868.06
June	829.48	887.35	925.93
July	733.02	848.77	868.06
August	675.15	694.44	733.02
September	501.54	617.28	655.86
November	347.22	424.38	462.96
October	231.48	270.06	308.64
December	177.47	185.19	231.48

Table 3.5: The annual average temperature for Istanbul, Ankara and Adana

Temperature/ Month	Istanbul Average Temperature (C)	Ankara Average Temperature (C)	Adana Average Temperature (C)
January	4	-1	10
February	6.5	1	11
March	8	5	13.5
April	11	10	17
May	16	14	21.5
June	22	19	25
July	22.5	21.5	27
August	22.5	21.5	29
September	20.5	18.5	27
November	15	12	21.5
October	11.5	7.5	16
December	7.5	3	12

Table 3.6: Definitions of Parameters

Parameters	Definitions
I_1, V_1	Initial current and voltage in the STC conditions
I_2, V_2	Secondary current and voltage according to the new radiation and temperature systems
G_1	The irradiance measured with the reference device
G_2	The irradiance at the standard or other desired irradiance
T_1	The measured temperature of the test specimen
T_2	The other desired temperature
I_{SC}	The measured short-circuit current of the test specimen at G_1 and T_1
α & β	The current and voltage temperature coefficients
R_S	The internal series resistance of the test specimen
k	The curve correction factor

Table 3.7: The temperatures of panels for Istanbul, Ankara, and Adana

Panel T(C)/ Month	Panel Ave. Temperature in Istanbul	Panel Ave. Temperature in Ankara	Panel Ave. Temperature in Adana
January	10.19	8.28	19.90
February	18.88	15.86	26.48
March	25.33	24.81	33.93
April	33.29	34.14	41.76
May	42.00	41.24	49.36
June	48.62	47.48	54.72
July	46.03	48.74	54.86
August	44.17	43.79	52.53
September	36.59	38.31	48.05
November	26.14	25.62	36.36
October	18.93	16.16	25.90
December	13.19	8.94	19.43

Table 3.8: The current of panels for each month

Max Current/Month	Panel Current in Istanbul (A)	Panel Current in Ankara (A)	Panel Current in Adana (A)
January	0.02	0.11	0.14
February	0.22	0.3	0.33
March	0.39	0.47	0.49
April	0.55	0.61	0.64
May	0.68	0.72	0.75
June	0.71	0.76	0.81
July	0.60	0.73	0.75
August	0.54	0.56	0.61
September	0.36	0.48	0.53
November	0.19	0.27	0.32
October	0.06	0.10	0.15
December	0.002	0.006	0.06

Table 3.9: The max voltage of panels per month

Max Voltage/Month	Panel Voltage in Istanbul (V)	Panel Voltage in Ankara (V)	Panel Voltage in Adana (V)
January	29.38	28.66	28.39
February	27.81	27.24	26.98
March	26.55	25.96	25.71
April	25.28	24.82	24.60
May	24.30	24.01	23.77
June	24.08	23.64	23.27
July	24.85	23.93	23.72
August	25.32	25.17	24.79
September	26.73	25.82	25.43
November	28.03	27.44	27.03
October	29.00	28.73	28.33
December	29.47	29.46	29.00

Table 3.10: Power values for one panel for each month

Max Power/Month	Panel's Power in Istanbul (w)	Panel's Power in Ankara (w)	Panel's Power in Adana (w)
January	0.45	3.24	4.07
February	6.17	8.13	8.85
March	10.26	12.09	12.70
April	13.98	15.22	15.74
May	16.52	17.26	17.74
June	17.00	18.07	18.86
July	15.01	17.36	17.81
August	13.74	14.15	15.11
September	9.54	12.34	13.38
November	5.29	7.35	8.57
October	1.83	2.88	4.21
December	0.06	0.19	1.84

Table 3.11: Energy values for one panel per month

Energy per day/ Month	Average Energy production in Istanbul (Wh)	Average Energy production in Ankara (Wh)	Average Energy production in Adana (Wh)
January	3.25	23.31	29.30
February	44.42	58.57	63.74
March	73.91	87.03	91.42
April	100.60	109.57	113.31
May	118.91	124.24	127.70
June	122.34	130.10	135.81
July	108.06	125.016	128.25
August	98.92	101.89	108.82
September	68.72	88.83	96.35
November	38.08	52.88	61.72
October	13.15	20.73	30.34
December	0.46	1.33	13.24

Table 3.12: LiFePO4 Specification

specific energy	90-110 Wh/kg (320-400 J/g)
Energy density	220 Wh/L (790 kJ/L)
Specific power	>300 W/kg
Energy/Consumer-price	0.5-2.5 Wh/US(US0.11-0.56/kJ)
Time durability	>10 years
Cycle durability	2,000 cycles
Nominal cell voltage	3.2 V
Max charge voltage	3.65 V
Min discharge voltage	2.75 V

Chapter 4

Results and Discussion

Three a-Si PV panels in this study, which are connected in parallel will be discussed. Second, the way that the results from panels are used in order to program the system for batteries performance evaluation will be explained. At the end, the overall system performance will be analyzed.

4.1 PV Calculation Results

Three a-Si PV panels in this study, are conected in parallel. The effect of temperature and solar radiation on panels in Istanbul, Ankara, and Adana are considered. Graphs below show the sequence of the three a-Si panels PV calculation results. Figures 4.1 , and 4.2 show the solar radiation and average temperatures in Istanbul, Ankara, and Adana [10]. Clearly by increasing solar radiation in each month, environment temperature is increasing as well. Also by looking further to the graphs, Ankara shows to have lower environment temperature, even though it has higher solar radiation from Istanbul in most of months of year.

Based on the data in Figures 4.1 and 4.2 the temperature of the panels were calculated. Figure 4.3 shows each panel's working temperature. The temperature of panels are increasing from January to June then decreasing from July to December. The intersting point in this graph is that panels in Ankara would have lower working temperature while they have higher solar radiation than Istanbul. The reason is that environment temperature is higher in Istanbul than in Ankara. This issue directly affect the efficiency of

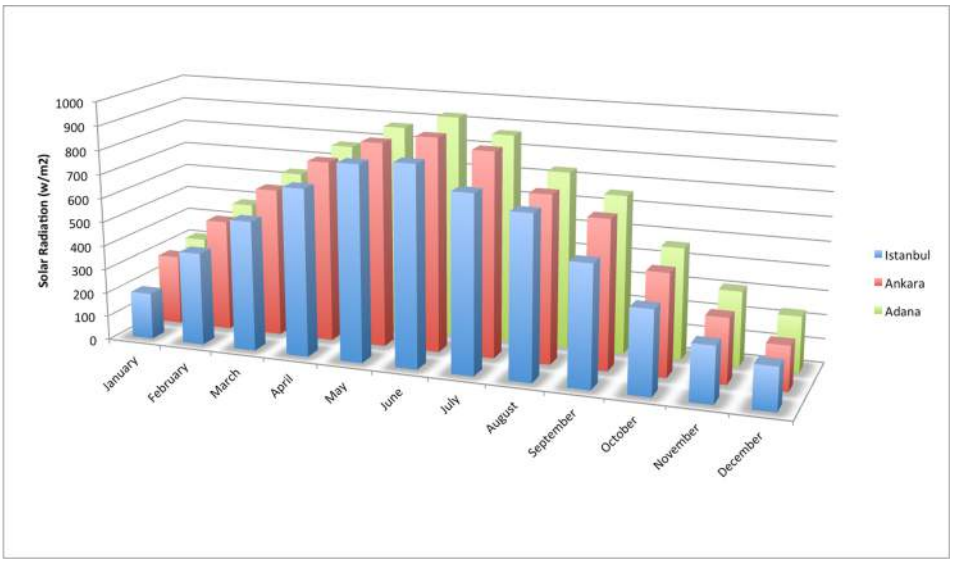

FIGURE 4.1: Annual solar radiation in Istanbul, Ankara, and Adana

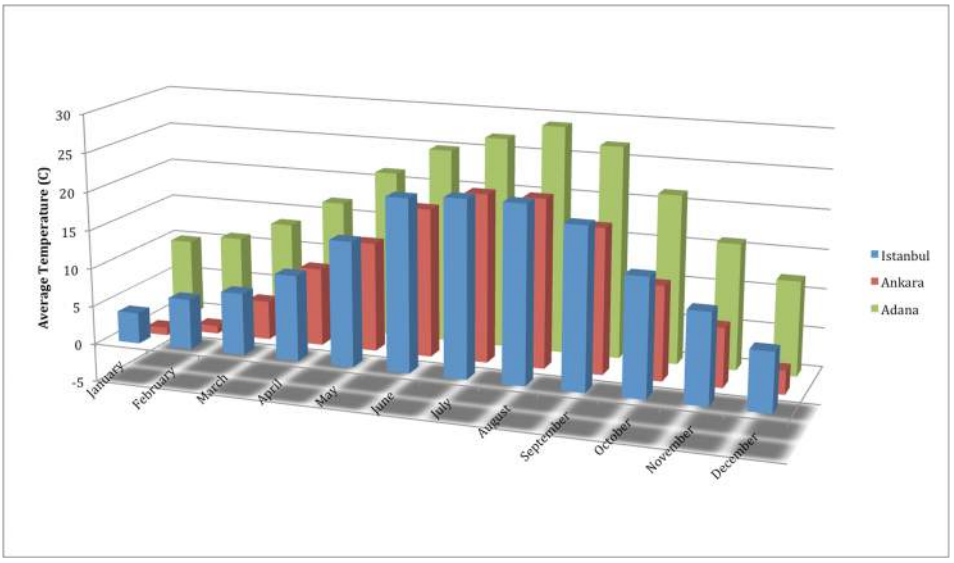

FIGURE 4.2: Annual environment temperature in Istanbul, Ankara, and Adana

panels in Ankara. On the other hand, Adana has the higher solar radiation, environment temperature and panel temperature among these three cites.

Based on Equations 3.8 and 3.9 average current and average voltage of panels are calculated by inserting obtained data from Tables 3.3, 3.4 and 3.5 into translation formulas. Figures 4.4 and 4.5 show the provided average current and average voltage of the panels. As it was anticipated the guaussian shape graph is obtained for current curve but voltage graph has different trend. Figure 4.5 has concave curve which shows different impact of temperature and solar insulation on this graph.

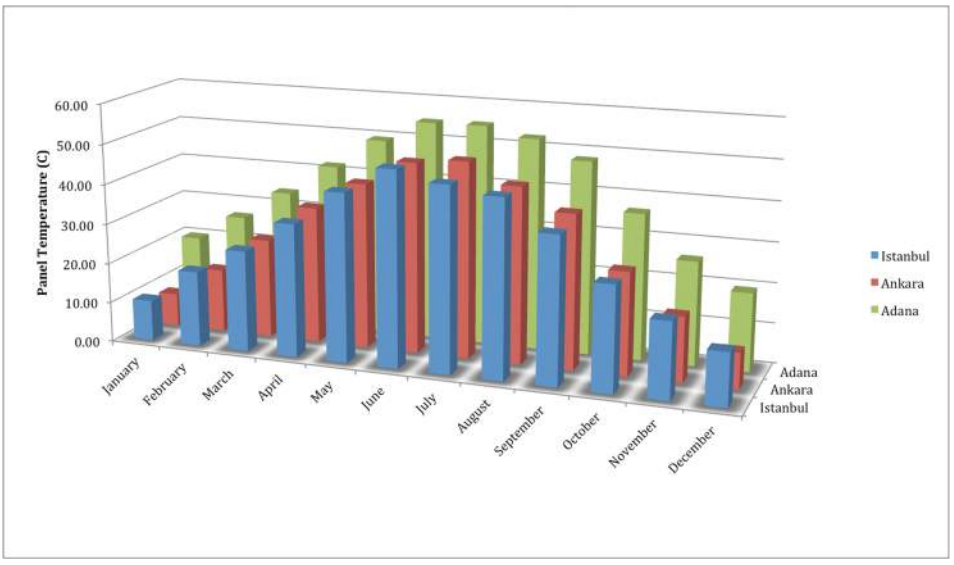

FIGURE 4.3: Annual average temperature for each panel in Istanbul, Ankara, and Adana

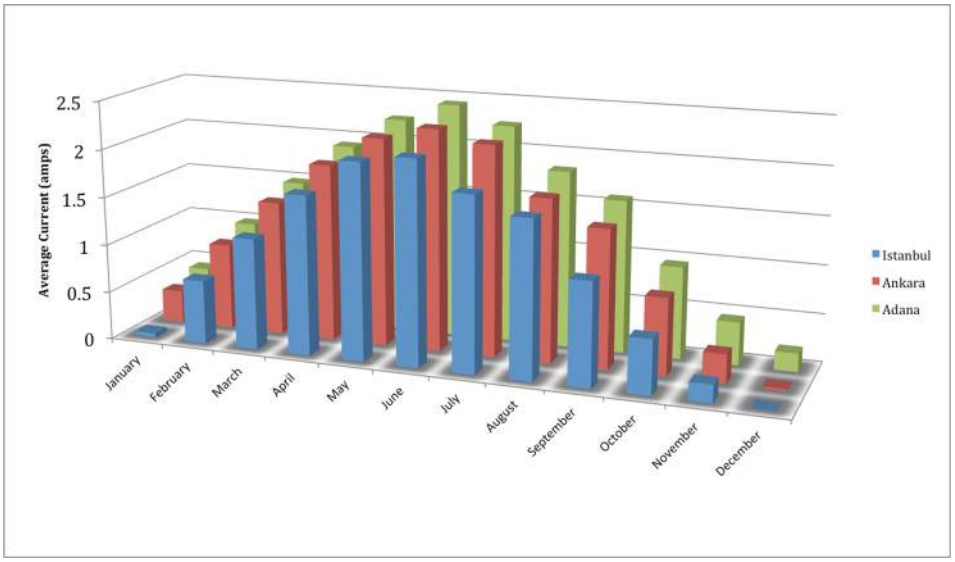

FIGURE 4.4: Annual average current for three panels in Istanbul, Ankara, and Adana

Based on Figures 4.4 and 4.5, Figure 4.6 is calculated for time period of a year for the three mentioned cities. It is showing the amount of power that can be delivered by the PV system in this investigation. The power delivery of the system in some months like January and December for Istanbul and in December for Ankara is almost ignorable. However the graph kept its bell shape style and in peak months like May, June and July the power delivery is noticeable. Among these three cities Adana has the highest power delivey for this PV system.

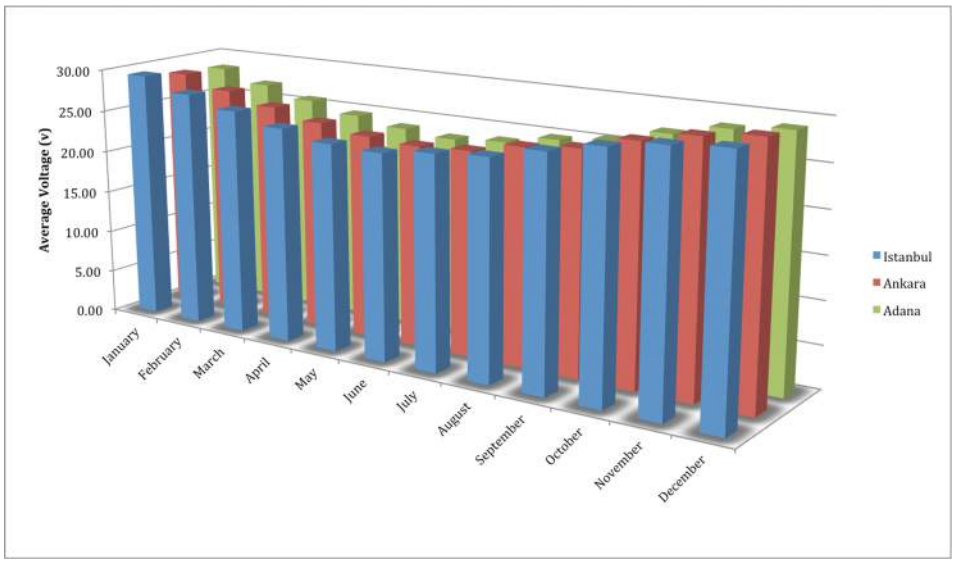

FIGURE 4.5: Annual average voltage for three panels in Istanbul, Ankara, and Adana

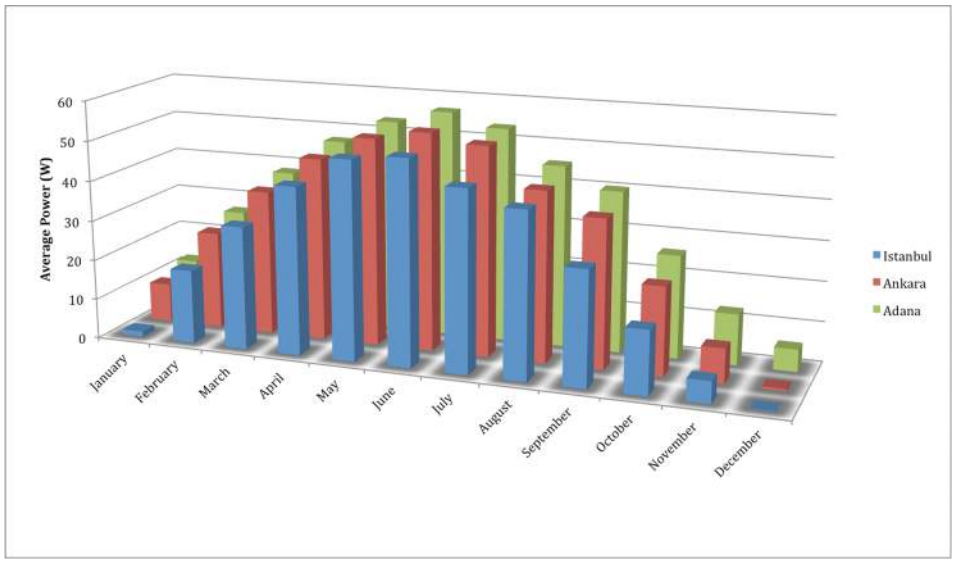

FIGURE 4.6: Annual average power for three panels in Istanbul, Ankara, and Adana

The yearly average solar radiation is $1311 kWh/m^2$per year and $3.6 kWh/m^2$ per day. The total yearly insulation period is approximately 2460 hours per year and 7.2 hours per day. Therefore, by multiplying this average insulation hours value with power values, energy (Wh) values are measured for the same cities. Figure 4.7 is showing the energy values in a sequence of a year for these three cities.

According to the Figure 4.7 the average available energy by these three a-Si panels is determined. As it is seen in the energy graph, months with low amount of power also deliver low amount of energy. In next step, power values are inserted to a program

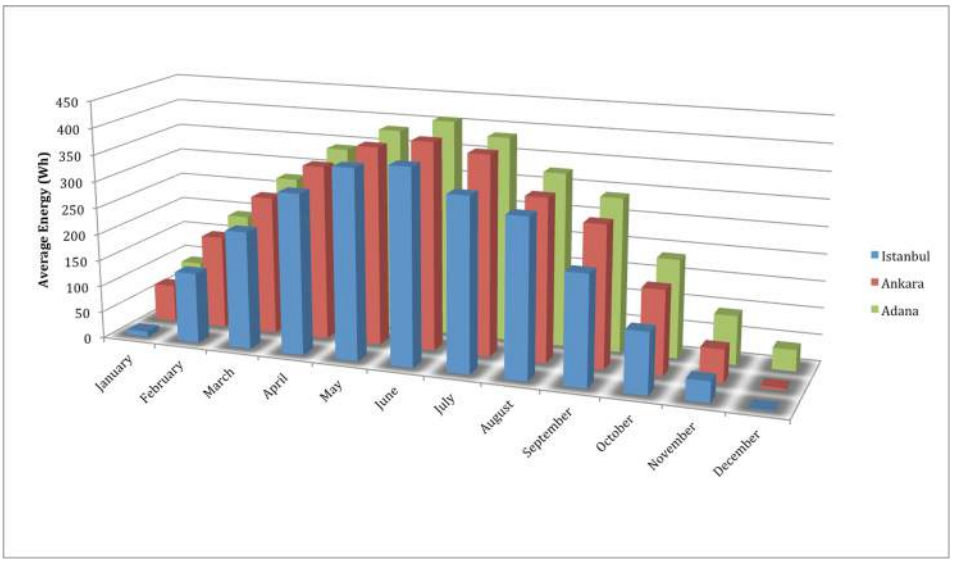

FIGURE 4.7: Annual average energy for three panels in Istanbul, Ankara, and Adana

in order to simulate the solar radiation. The solar simulator system is connected to the LiFePO4 battery package. Charging and discharging processes by considering the inserted power to the solar simulater is done by battery tester. The interesting point is that both Figures 4.4 and 4.6 are concave graphs while Figure 4.5 has a convex trend. This reason of this issue will be discussed in the discussion section.

4.2 System Outputs

In this study each package of battery is contained five parallel cells, and 8-battery package were connected in series. The battery theoretical calculations were provided in the previous chapter. In this section, first, in order to give an idea how the calculated data are inserted to the program, one specific interface of battery tester software will be presented for each of the cities. Second, the LiFePO4 battery packages performance will be presented. Figures 4.8 , 4.9 and 4.10 show two full steps of inserting Istanbul, Ankara, and Adana's power values of January and February to the Digatron Firing Circuits software.

Each iteration has three steps. The first step is designed as pause with standard time value of 2 minutes and limit of 10 minutes. The second step is charging with inserting power values as input. Power values are coming from Figure 4.6, are chosen as nominal input value for these three cities. There were three limits for charging steps. First, 7.2h as charging time, which was coming from effective solar irradiation hours per day

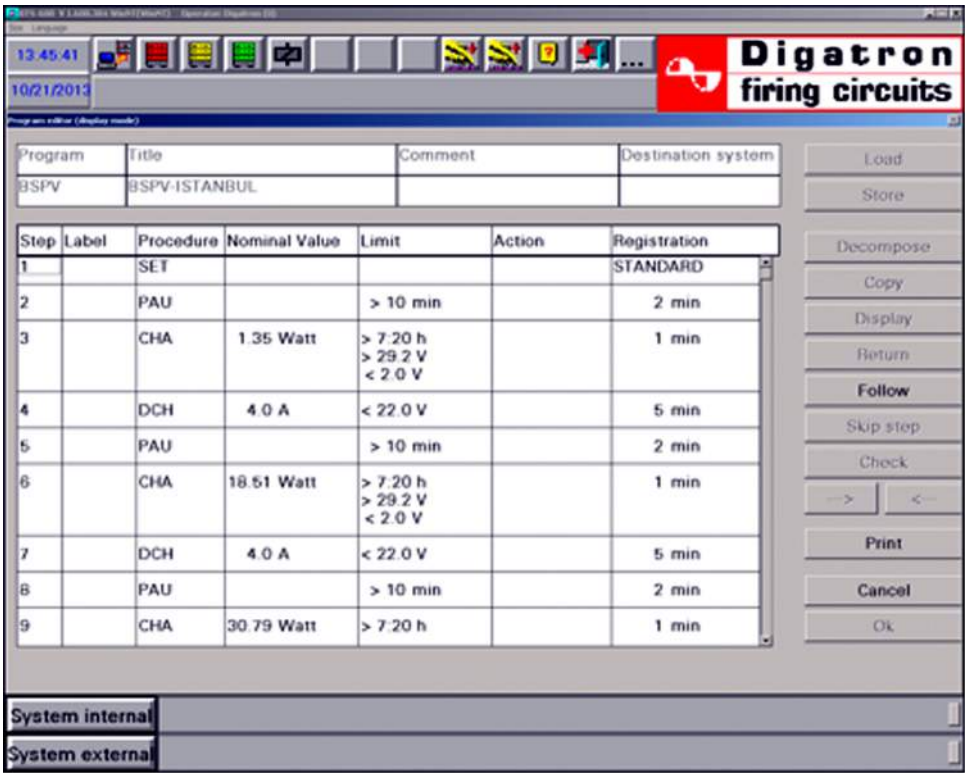

FIGURE 4.8: An interface of Digatron Firing Circuits software for Istanbul

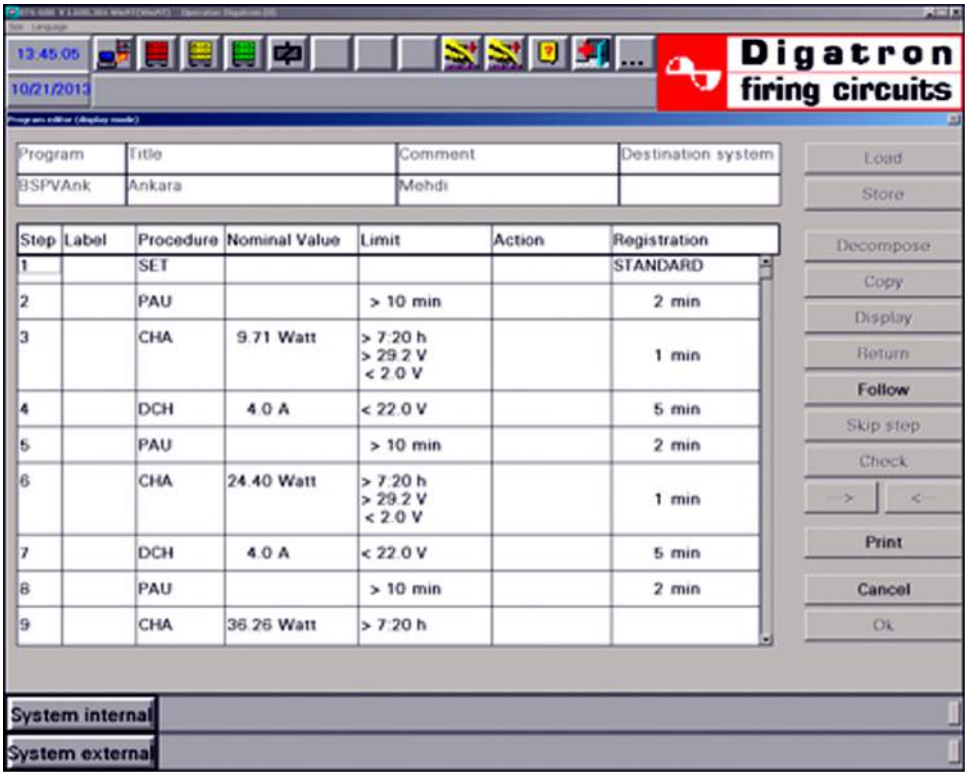

FIGURE 4.9: An interface of Digatron Firing Circuits software for Ankara

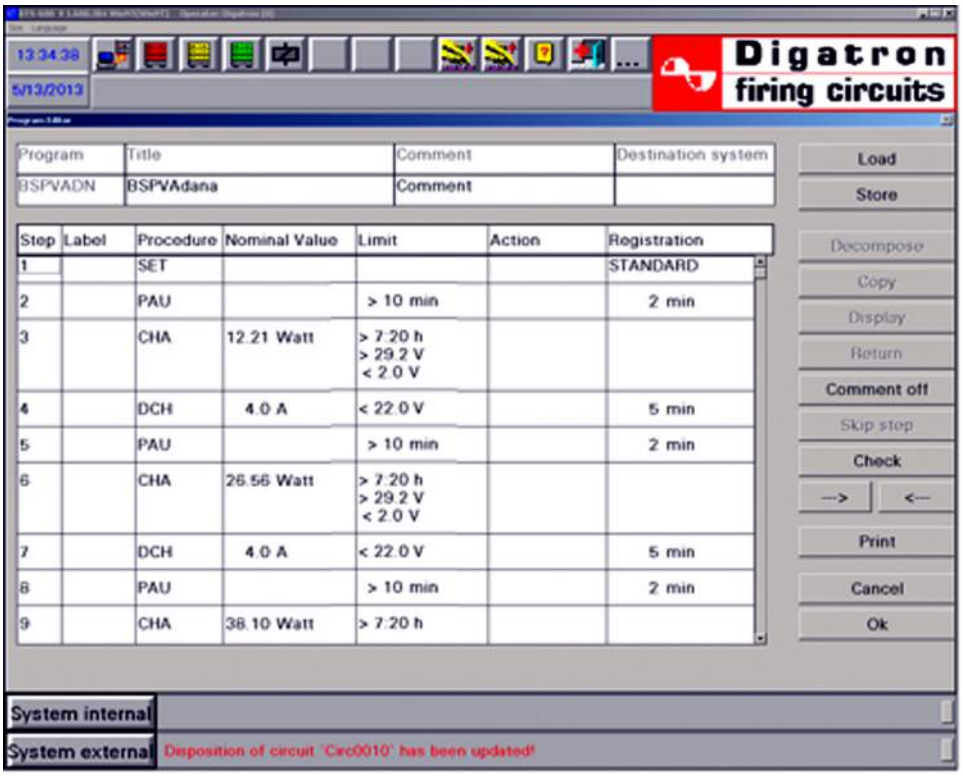

FIGURE 4.10: An interface of Digatron Firing Circuits software for Adana

assumed in this study, second, max and min voltage of batteries which are 29.2 and 2V respectively. Max and min voltage of batteries are coming from high power LFP battery specifications. Eventually the last step is the discharging. In this step, 4A is inserted as discharging current with a limit of 22V. This limit also is coming from battery minimum discharge voltage specifications. As it can be seen in these three sample interfaces, Figures 4.8 , 4.9 and 4.10 all the inserted values during pause, charging and discharging steps for two iterations of January and February are visible.

After inserting all the calculated power values into the program and considering all the limits, which were coming from battery specifications, the system ran for several days continuously until the final results in format of excel file were gathered. Figures 4.11, 4.12, and 4.13 show energy and voltage charge and discharge graphs versus each month for a time sequence of one year for three cities of Istanbul, Ankara, and Adana. Each rising line is showing charge process and falling lines are showing dis-charging processes. The details will be discussed in the discussion section.

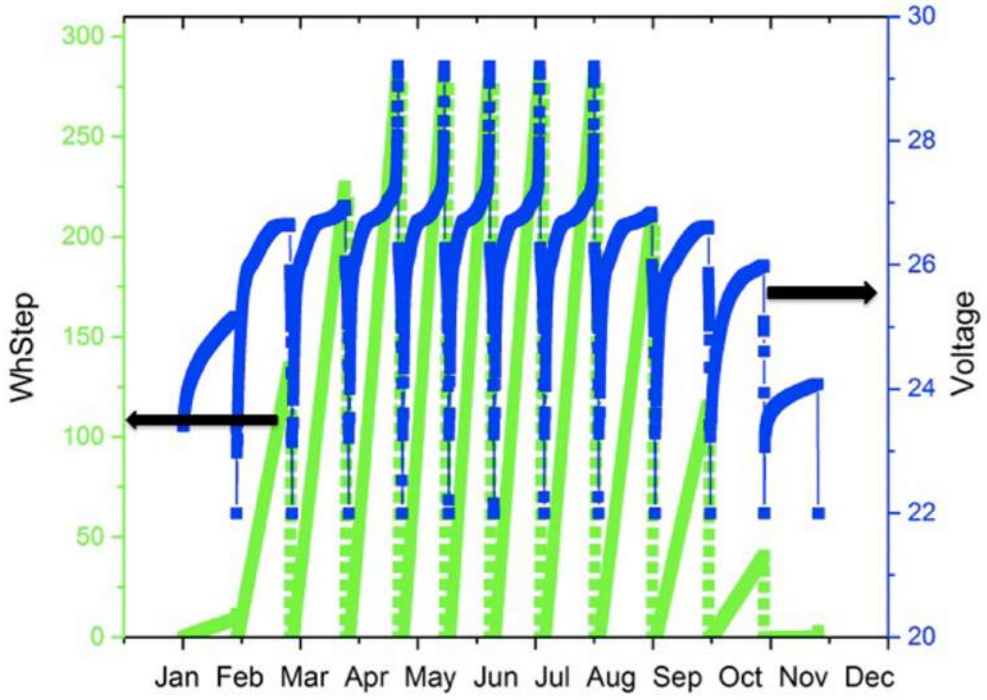

FIGURE 4.11: Battery tester result for Istanbul

4.3 Discussion

In this section first graphs of a-Si panels will be discussed, and then graphs of LiFePO4 batteries, which are presented, in the result section will be discussed.

4.4 A-Si Panel Results

During this study temperature and solar radiation effects were considered on three a-Si panels with an efficiency of 7%. Translation equations and mentioned fomulas in previous chapter are used to come up with current and voltage of cells after exposing to sunlight and increasing the temperature of panels. In order to do these three cities were chosen, and their average solar radiation and ambient temperature for time sequence of one year were recorded. The reason Istanbul, Ankara, and Adana were chosen, was to have three different solar irradiation and ambient temperature sets with reasonable differences. As it

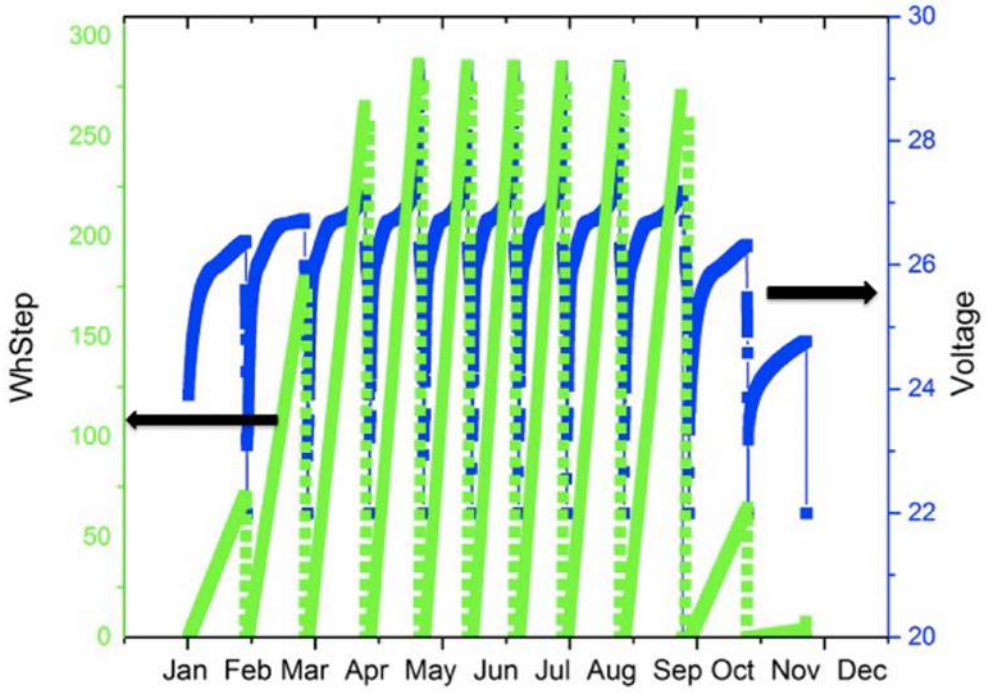

FIGURE 4.12: Battery tester result for Ankara

can be seen in the Figures 4.1 and 4.2 the average solar radiation and average temperature are represented, and the differences among the sets are practical for each of these figures. According to Figure 4.1 Istanbul has the lowest solar irradiation among the three cities and Adana has the highest amount of irradiation. It is significant to mention even during the highest radiation months, which are May, June, and July still the differences are totally sensible among the three cities. Also temperature differences are completely clear for these three cities according to Figure 4.2. By using this basic information, which is coming from recorded data from the weather forecasts for more than 20 years, the study was started. In the first step of the calculations, it was necessary to determine cells working temperature by using Equation 3.6. The results are represented in Figure 4.3. The interesting point here is the difference between ambient temperature and working temperature of panels. In almost all of the cases the panel's working temperature is more than two times the ambient temperature. Figures 4.2 and 4.3 are clearly showing these differences.

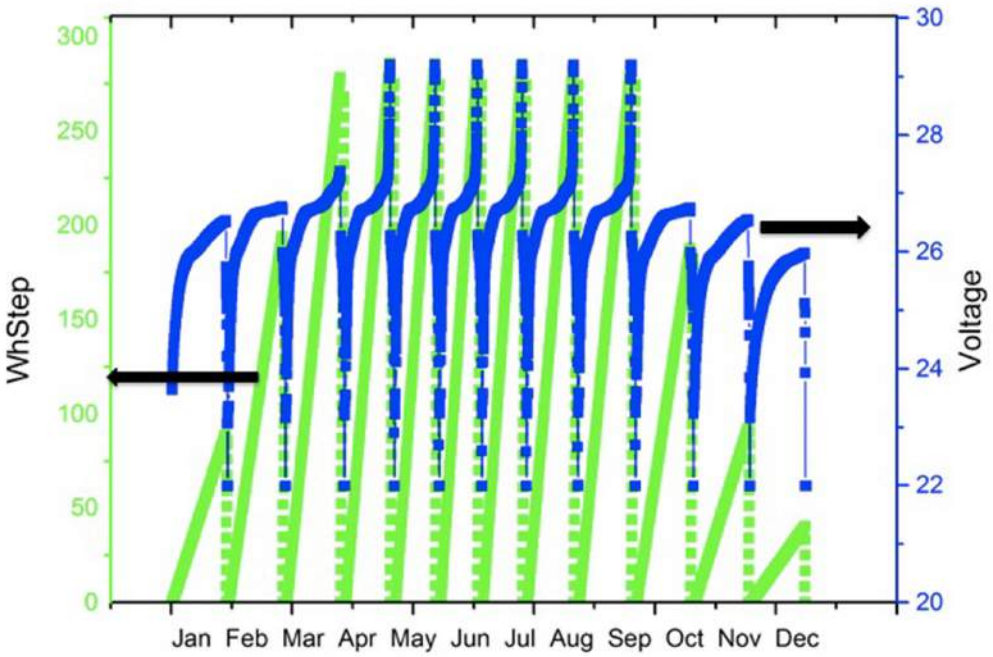

FIGURE 4.13: Battery tester result for Adana

By clarifying the panel's working temperature, and using panel's specifications to determine α and β everything for calculating average current and voltage of the panels is ready by using Equations 3.8 and 3.9. In Equation 3.9 the second part effect is negligible that is why the factor k which is curve correction factor, is considered as zero. In the same equation R_s is considered as 7.5 Ω according to the manufacturer specifications for the panels. The results of these formulas are represented in Figures 4.4 and 4.5. The point about these graphs is that in Figure 4.4 by increasing the solar irradiation and temperature the current is increasing until June and then again by decreasing of solar irradiation and temperature the current decreased. However, in Figure 4.5 the gradient is not going the same as average current graph. Even though the solar irradiation is increasing the voltage is decreasing. This shows that the negative effect of temperature outweigh positive effect of solar irradiation. That is why the slope of Figure 4.5 until the peak month, which is June, is decreasing and after that it is increasing.

Power value calculations are done for the next step by using equation below.

$$P = V \times I \tag{4.1}$$

Figure 4.6 is showing the power values for each of the three cities for a time sequence of one year. Therefore, this is the average power value that three a-Si panels in this study can provide in each month. A Gaussian graph is resulted from the multipication of calculated current and voltage amounts, even though voltage has a concave graph. As it is known, if the radiation is constant, increasing temperature decreases the efficiency. Figure 4.14 shows effect of temerature on the efficiency of photovoltaic panels [23]. Therefore, it is concluded the effect of radiation outweight the negative effect of temperatue on voltage.

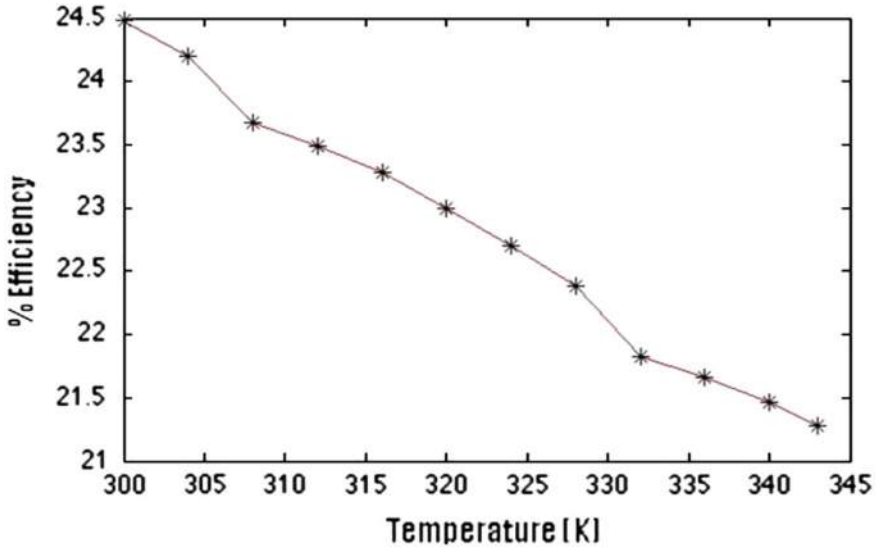

FIGURE 4.14: Effect of temperature on efficiency

As it is mentioned before 7.2 hours is considered as the average effective solar irradiation hours for each day in Turkey. Therefore, by multiplying this number to power values the energy values are calculated Figure 4.7. By looking to the graph, at first glance it is quit visible that the amount of provided energy by panels is not sufficient in months such as January, October, and December. Therefore, in the application this should be considered.

4.5 LiFePO4 Results

By inserting the power values and battery specifications and considering 7.2 hours as the effective irradiation time per day into the Digatron software, Figures 4.11, 4.12 , and 4.13 are resulted.

According to the left side vertical axes the graphs are showing energy that batteries can store and discharge in each month. Also according to the right side axes in these graphs, voltage for each charge and discharge sequence is shown. However, for clarifying the situation a bit more, for Adana one charge and discharge sequence is shown in detail in Figure 4.15. This graph is drawn based on the provided data for one day in month June.

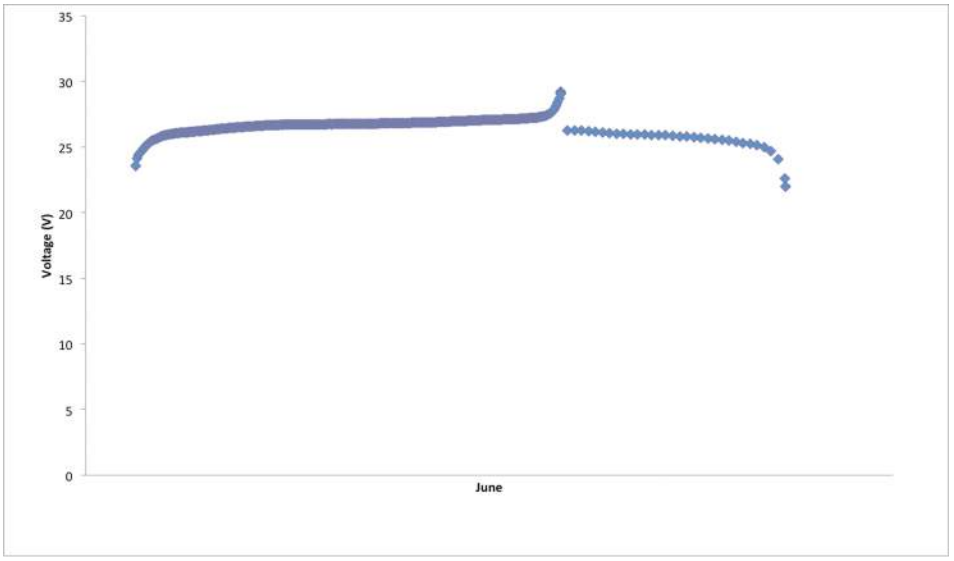

FIGURE 4.15: The voltage charge and discharge in June for Adana

On the other hand, in order to get more in depth for energy graphs, capacity graphs are also added to this section. Figures 4.16, 4.17 and 4.18 are showing the LFP batteries results in sequence of one year. As it is anticipated, Adana has the best results with seven peak months from March to September with capacity value between 10-12Ah, after that Ankara has the highest number of peak months with capacity values among 10-11Ah and eventually Istanbul has five peak months with values of more than 10Ah.

According to Figure 4.11 there is no energy charge and discharge for December, however figure 4.16 shows a small capacity charge. The point here is that at the beginning the battery cycler started to charge batteries for very short time but after a while the limit of voltage stopped the sequence of steps in this month. Also the same scenario happened for November and December for Ankara results with considering this difference that in December no charging process even started for Ankara.

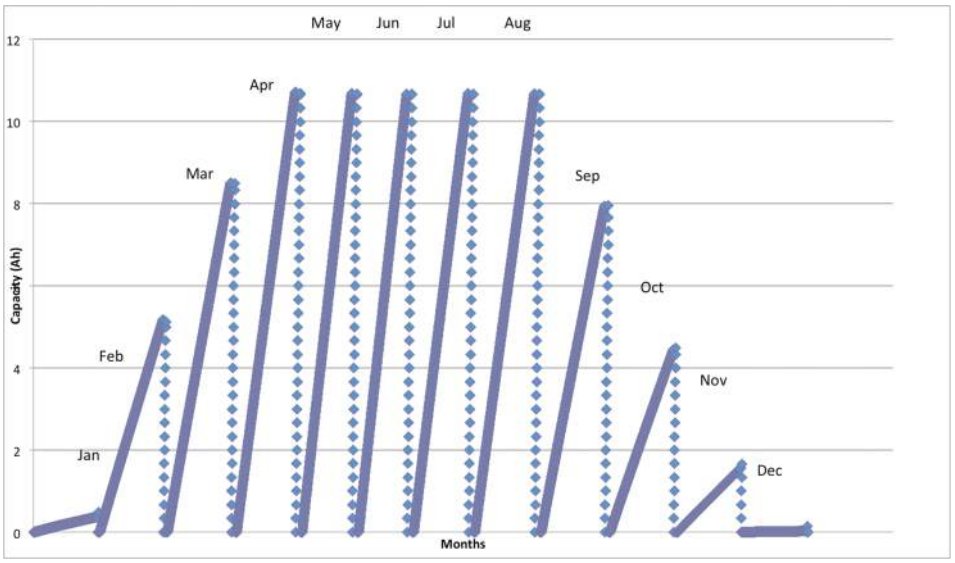

FIGURE 4.16: Istanbul's capacity outputs for each month

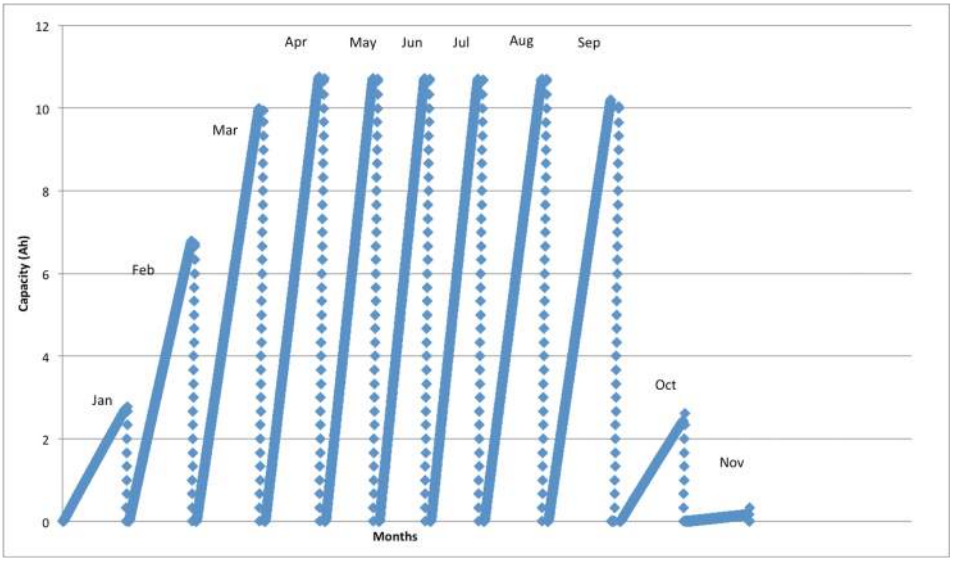

FIGURE 4.17: Ankara's capacity outputs for each month

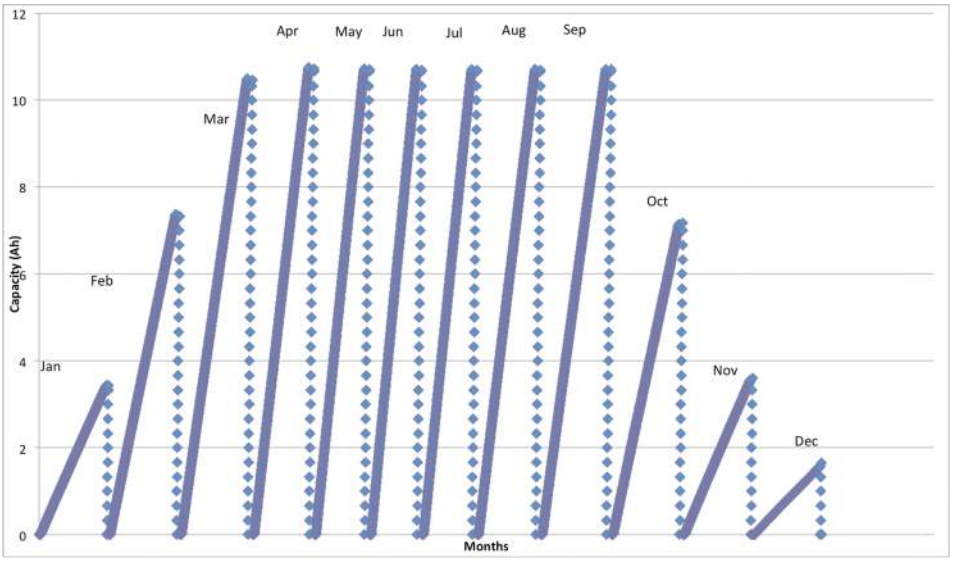

FIGURE 4.18: Adana's capacity outputs for each month

Chapter 5

Conclusion

In this study a battery based stand-alone system was designed. The electricity generation portion was a three a-Si panel system connected in parallel and for storage a LFP battery was used. The high power LFP battery packs are 40 cells each 8S5P (configured 8 series 5 parallel). Each individual pack weighed 0.5 kg and is 25.6V. Istanbul, Ankara and Adana were chosen in order to evaluate the effect of temperature and solar irradiation on the a-Si panels' efficiency. Temperature and solar irradiation were gathered from reliable sources and by using translation equations, current and voltage output of panels were calculated. As a result of these calculations, power and energy outputs were calculated by considering 7.2 h as an average efficient solar irradiation time value per day in Turkey.

The power values were inserted in the battery cycler computer-based program. The system was connected to a UBT (universal battery tester). The high power LFP batteries were put in the UBT in order to test their behavior with regard to the provided data in the program. The test was run for the three cities. It took four, five, and six days for Istanbul, Ankara, and Adana to complete the simulation tests respectively. Each charging steps took 7.2 hours and it was followed with a discharge step. The duration of discharge steps were different based on the amount of stored energy in the batteries. The next step was a 10 minutes pause. This procedure was done for a sequence of one year for each month.

Figures: 4.11, 4.13 analysis are showing promising results for a couple of months. For each city the number of peak months and the amount of energy storage is different. According to the results, the highest values of energy are stored in Adana, it followed

by Ankara and then Istanbul. The results are in a good agreement with what was anticipated from the solar irradiation amount and temperature of cities. Adana has the highest amount of solar irradiations and environment temperature, and the next one is Ankara and followed by Istanbul.

5.1 Future Research and Recommendations

In general, this study can be a beginning for further investigations in this area. A couple of assumptions were considered in this investigation that could increase the possibility of errors. Assumptions like the resistance value R_s in equation 3.8, correction factors in equation 3.9 , T_{NOCT} and $C(t)$ in equation 3.6 have enough room to be investigated in order to come up with more precise results.

Therefore, it is suggested that these factors should be considered in future studies. Also different photovoltaic materials with higher efficiencies can be modeled based on this study with the same procedure. The main reason that in this study amorphous silicon was chosen is its low price and the availability of this material. Furthermore, performance of other batteries can be investigated as well. For different applications and cities, different batteries may be useful. In addition, the effect of temperature on battery efficiency and battery aging are parameters that can be further investigated. The effect of a sun tracker system for the solar panels can be considered and in case, it is possible to consider the optimization of a system with low solar panel efficiency with sun tracker system rather than using high efficiency PV materials for solar panels. Also when it comes to installation of the system there are several other issues that should be considered. Issues such as wire type and sizing, switches and fuses, connections, system installation, grounding, and eventually maintenance should be optimized in order to develop the highest efficiency.

In summary, it is possible to optimize the use of a BSPV for each location and application.

Note: Chapter 3 of this thesis is partially coming from the author published article [23].

Bibliography

[1] *Status, Trends, Challenges and the Bright Future of Solar Electricity from Photovoltaics*, chapter 1. WILEY, 2003.

[2] D. Carlson and C. Wronski. Amorphous silicon solar cell. *Appl. Phys. Lett.*, 1976.

[3] J. Yang, A. Banerjee, and S. Guha. Triple-junction amorphous silicon alloy solar cell with 14.6and 13.0 *Appl. Phys. Lett.*, 1997.

[4] M. Vanecek, A. Poruba, Z. Remes, N. Beck, and N. Nesladek. Optical properties of microcrystalline materials. *J. Non-Crystalline Solids*, 1998.

[5] *LiFePO4 Cathode Material, Electric Vehicles: The Benefits and Barriers*, chapter 11. Intech, 2011.

[6] X. Wang, P. Adelmanna, and T. Reindla. Use of lifepo4 batteries in stand-alone solar system. *Energy Procedia*, 2012.

[7] *Photovoltaic Systems: Handbook of Photovoltaic Science and Engineering*, chapter 17. Wiley, 2003.

[8] N. Jenney. *Photons In, Electrons Out: Basic Principles of PV*. 2010.

[9] I. Buchmann. Types of lithium-ion, 2013. URL `http://batteryuniversity.com/learn/article/types_of_lithium_ion`.

[10] H. Bulut and O. Buyukalaca. Simple model for the generation of daily global solar-radiation data in turkey. *Applied Energy*, 2007.

[11] C. Fritts. New form of selenium photocell. In *Proc. Am. Assoc. Adv. Sci.*

[12] D. Chapin, C. Fuller, and G. Pearson. A new silicon p-n junction photocell for converting solar radiation into electrical power. *J. Appl. Phys.*, 1954.

[13] E. Williams. The physics and technology of xerographic processes. *Wiley*, 1984.

[14] J. Mort. The anatomy of xerography: Its invention and evolution. *McFarland, Jefferson, NC*, 1989.

[15] D. Adler R. Chittick, H. Sterling and H. Fritzsche. Tetrahedrally bonded amorphous semiconductors. *Plenum Press, New York, NY*, 1985.

[16] W. Spear and P. LeComber. Amorphous and liquid semiconductors. *Solid State Commun.*, 1975.

[17] J. Perlin. The story of solar electricity. *aatec Publications, Ann Arbor*, 1999.

[18] M. Archer C. Wronski, D. Carlson and R. Hill. Clean electricity from photovoltaics. *World Scientific*, 2001.

[19] H. Fritzsche. Hydrogen content and density of plasma deposited amorphous silicon-hydrogen. *Mater. Res. Soc. Symp. Proc.*, 2001.

[20] A. G. Ritchie. Recent development and future prospects for lithium rechargeable batteries. *Journal of power Sources*, 2001.

[21] Y. Gao and J. R. Dahn. Synthesis and characterization of $li_{1+x}mn_{2-x}o_4$for lithium ion battery application. *Journal of Electrochemical Society*, 1996.

[22] A. K. Padhi, K. S. Nanjundawamy, and J.B. Goodenough. Photo-olivines as positive electrode materials for rechargable lithium batteries. *Journal of Electrochemical Society*, 1994.

[23] M. H. Vishkasougheh and B. Tunaboylu. Simulation of high efficiency silicon solar cells with a hetero-junction microcrystalline intrinsic thin layer. *Energy Conversion and Management*, 2012.

[24] Unknown. World weather and climate information, 2013. URL `http://www.weather-and-climate.com/average-monthly-Rainfall-Temperature-Sunshine-in-Turkey`.

[25] A. C. McEvoy. Factors that influencing the diffusion of solar energy technologies in turkey. Master's thesis, European Master in society, Science and Technology, 2001.

[26] C. Kick. How is 100 percent renewable energy possible for turkey by 2020. Technical report, Gelobal Energy Network Institute, 2011.

[27] O. Coban and F. Nur Yorgancilar. Relationship between renewable energy consumption and sustainable economic growth: The case of turkey. In *The 2011 Barcelona European Academic Conference*.

[28] M. Mayer. Why are solar cells made of silicon, 2012. URL `http://berc.berkeley.edu/why-are-solar-cells-made-of-silicon_1/`.

[29] Q. Wang, M. Page, E. Iwaniczko, X. Yueqin, L. Roybal, and et al R. Bauer. Efficient heterojunction solar cells on p-type crystal silicon wafers. 2010.

[30] *High efficiency a-Si:H/c-Si heterojunction solar cells*, 1994.

[31] H. Hamadeh. Temperature dependence of pin solar cell parameters with intrinsic layers made of pm-si:h and low crystalline volume fraction mc-si:h. *Renewable Energy*, 2010.

[32] Y. Hishikawa, Y. lmura, and T. Oshiro. Irradiance-dependence and translation of the i-v characteristics of crystalline silicon solar cells. *IEEE*, 2000.

[33] T. Schroer. Digatron firing circuits, 2013. URL `http://www.digatron.com/nc/en/home/`.